Bachofer *et al. Anthropocene Coasts* (2026) 9:1
https://doi.org/10.1007/s44218-025-00109-6

Anthropocene Coasts

RESEARCH ARTICLE

Open Access

Urban growth prediction along Shared Socioeconomic Pathways (SSPs) for future flood exposure risk assessment: a cross-continental analysis of coastal cities

Felix Bachofer[1*], Zhiyuan Wang[1], Juliane Huth[1], Christina Eisfelder[1], Andrea Reimuth[2] and Claudia Kuenzer[1,3]

Abstract

Climate change remains a defining challenge of the twenty-first century, profoundly impacting ecosystems, economies, and human settlements. Among its consequences, the intensification of flood risks in coastal cities poses a critical threat to sustainable development, particularly in the Global South. This study bridges climate change-induced flooding scenarios with urban growth modelling, integrating Shared Socioeconomic Pathways (SSPs) into the SLEUTH model to simulate future urban trajectories and assess flood exposure under varying climate and socioeconomic conditions. Leveraging Earth observation information products, flood hazard scenarios based on Representative Concentration Pathways (RCPs) and high-resolution (30 m) urban growth projections, this study evaluates coastal, fluvial, and pluvial flood exposure for nine coastal agglomerations with diverse socioeconomic and environmental contexts. Urban growth projections under SSP1/RCP2.6, SSP2/RCP4.5, and SSP5/RCP8.5 scenarios reveal significant variability in urban expansion rates, with four cities projected to expand by over 50% by 2050. Flood exposure assessments for the target year 2050 reveal nuanced spatial and scenario-dependent patterns across all flood types: Surabaya (Indonesia) faces severe coastal flooding (up to 83 km^2 under SSP5/RCP8.5), while Guayaquil (Ecuador) and Ho Chi Minh City (Vietnam) experience extensive risks of fluvial flood exposure, with over 37% of newly developed areas inundated in Guayaquil. Notably, the SSP2/RCP4.5 "Middle of the Road" scenario yields the lowest flood exposure in Khulna (Bangladesh) and Surabaya, whereas SSP1/RCP2.6 and SSP5/RCP8.5 project 30% to over 70% higher exposure in these cities. Disproportionate exposure to inundation in newly urbanized areas, particularly for Dar es Salaam (Tanzania) and Guayaquil, underscores potential risks associated with rapid and uninformed urbanization into flood prone regions. These findings emphasize the dual role of high radiative forcing climate scenarios and socioeconomic pathways in shaping flood exposure and associated risks, advocating for integrated strategies that combine climate mitigation with proactive, scenario-based urban planning.

Keywords Urban growth modelling, Shared socioeconomic pathways (SSPs), Flood exposure, SLEUTH, Coastal urban areas, Climate change impacts

*Correspondence:
Felix Bachofer
felix.bachofer@dlr.de
Full list of author information is available at the end of the article

1 Introduction

Climate change is one of the most pressing challenges of the twenty-first century, with widespread impacts on ecosystems, economies, and human settlements (IPCC 2023). Among its many consequences, the intensification of flood risks in coastal cities is a major concern. Coastal and pluvial floods, driven by rising sea levels, shifting precipitation patterns, and more frequent extreme weather, threaten urban sustainability and resilience, particularly in the Global South (Glavovic et al. 2022). Historically, coastal cities have thrived as hubs of commerce, culture, and innovation, attracting populations seeking economic opportunities and a higher quality of life (Barragán and de Andrés 2015). However, rapid urbanization and climate change now heighten flood risks, requiring urgent attention. Coastal cities, often near seas and river estuaries, are at the forefront of climate-induced flooding (Hallegatte et al. 2013; Edmonds et al. 2020; Strauss et al. 2021). The impacts are multifaceted, ranging from immediate threats to life and property to long-term socioeconomic disruptions. Flood events often jeopardize critical infrastructure, disrupt supply chains, displace communities, and are undermining the social fabric of these cities (Dodman et al. 2023). Moreover, recurring floods perpetuate a cycle of damage and recovery that exacts a substantial toll on public finances and exacerbates the vulnerability of marginalized populations (Glavovic et al. 2022).

1.1 Settlement growth prediction: input data and tools

The scientific community has responded to this challenge by developing advanced modelling tools and methodologies to assess and predict flood exposure for urban environments (Hanson et al. 2010; Edmonds et al. 2020; Nicholls et al. 2021; Strauss et al. 2021). Integrating these tools with scenarios of future urban and settlement growth is imperative, as urbanization continues and (peri-)urban areas expand into flood-prone zones. These tools, along with accompanying research, have been bolstered by freely accessible, global, flood-related datasets for past events (Tellman et al. 2021), current floodplains (Nardi et al. 2019) and early warning systems (Alfieri et al. 2013). Key datasets delineating current and future coastal and riverine flood prone areas under integrated climate scenarios include the Fathom Global Flood Map (30 m resolution) (Hawker et al. 2022; Fathom 2023) and the World Resources Institute (WRI) Aqueduct Flood Analyzer maps (30×30 arc seconds resolution) (Winsemius et al. 2015, WRI Aqueduct 2023). In addition, Earth observation (EO) products have become vital for urban modelling, demonstrating immense potential for predictive analysis (Koehler and Kuenzer 2020). High-resolution global settlement extent maps from satellite imagery have revolutionized large-scale urban modelling. Datasets such as the Global Human Settlement Layer (GHSL) (Corbane et al. 2019; Florczyk et al. 2019), Global Annual Impervious Area (GAIA) (Gong et al. 2019, 2020), and Global Impervious Surface Area (GISA) (Huang et al. 2022) highlight the value of remote sensing-derived products for urban studies. Notably, the World Settlement Footprint (WSF) evolution dataset has further enriched the field, offering a yearly account of global settlement extents at 30 m resolution from 1985 to 2015 (Marconcini et al. 2019, 2021).

Urban or settlement growth modelling has become essential in future flood risk analysis. Simulating future urban growth scenarios offers a proactive approach to flood risk management (Li and Gong 2016). A diverse array of methods has been employed to predict future urban and built-settlement growth. Approaches such as the CLUE models (Verburg et al. 2002; Verburg and Overmars 2009; Srichaichana et al. 2019) and the Future Land Use Simulation (FLUS) model (Liu et al. 2017, 2022) are widely used for modelling land use and land cover changes, particularly within multi-class contexts. For urban development studies, Gao and O'Neill (2019) introduced the data-driven Spatially-Explicit, Long-term, Empirical City development (SELECT) model. Wang et al. (2022) transformed the spatial and temporal changes derived from annual settlement extent layers into a Spatio-Temporal Matrix (STM) for growth prediction with a multi-layer perceptron (MLP). Similarly, Wolff et al. (2020) applied an MLP trained on CORINE land cover data to map spatial probabilities of future urban growth in the Mediterranean. They combined a non-spatial urbanization model with GDP and population data from Shared Socioeconomic Pathways (SSP) scenarios at 100 m spatial resolution to estimate urbanized pixels and exposure to sea level rise. Based on this methodology, Wolff et al. 2023 analysed the projected urban extent by 2100 for the European Union member states. Moreover, cellular automata (CA) modelling (Li and Gong 2016; Musa et al. 2016; Yeh et al. 2021), known for its spatially explicit representation of urban growth, is widely applied. Among rule-based CA models, the SLEUTH model (Clarke et al. 1996, 1997) has gained widespread adoption in urban growth modelling (Wu et al. 2008; Rafiee et al. 2009; Feng et al. 2012; Kuo and Tsou 2017; Goncalves et al. 2019; Zhou et al. 2019; Clarke and Johnson 2020; Kumar and Agrawal 2022), and is characterized by its process-based approach and the ability to simulate policy scenarios. It has been a widely applied tool in the field of urban planning (Chaudhuri and Clarke 2013) and increasingly tested for flood exposure projections (Reimuth et al. 2023). It derives its name from its input variables: Slope, Land use, Exclusion, Urban, Transportation,

and Hillshade (Clarke et al. 1996) and allows to simulate spatially explicit urbanization patterns through five control parameters. Unlike models focused on land-use transitions (e.g., CLUE, FLUS), SLEUTH explicitly captures growth mechanisms such as edge expansion and road-influenced development.

1.2 Future socioeconomic scenarios in urban modelling

Projecting urban growth in a rapidly evolving world requires scenarios that encapsulate varying socioeconomic trajectories. The SSPs, introduced as a framework by the scientific community, provide a spectrum of plausible narratives for future societal development. The SSPs outline global trends, ranging from sustainable to fragmented development, capturing future changes in energy, population, environment, and land use/land cover throughout the twenty-first century (Riahi et al. 2017). Based on five qualitative scenarios, quantified data on population (Kc and Lutz 2017), degree of urbanization (Jiang and O'Neill 2017), and gross domestic product (GDP) (Leimbach et al. 2017; Crespo Cuaresma 2017; Dellink et al. 2017) have been developed and projected to 2100. However, integrating them into urban modelling remains a relatively new approach for understanding future urbanization dynamics.

Jones and O'Neill (2016) introduced a global population scenario framework aligned with the SSPs, employing a gravity-based downscaling model. Their approach ensures quantitative consistency with national population and urbanization projections aligning with SSP spatial development narratives. Merkens et al. (2016) introduced spatial projections for global coastal population distribution across the five SSPs, developing coastal-specific narratives that differentiate coastal and inland population dynamics in urban and rural areas. Terama et al. (2017) linked SSP-based national population projections to population distributions at European sub-national level. Their method integrates population allocation as a pivotal driver of residential urban demand, particularly emphasized in SSP5-based scenarios, influencing regional urban growth. Chen et al. (2020) simulated global urban land expansion under SSPs at a 1 km resolution in 10-year intervals from 2020 to 2100. Gao and O'Neill (2020) leveraged a data-science approach and 15 diverse datasets, including a 40-year global time series of remote sensing observations, to derive global urban land projections for the twenty-first century. Their findings suggest a potential 1.8–5.9fold increase in global urban land under various SSPs. Chen et al. (2022) utilized a logistic fitting model for updating global urbanization projections from 2015 to 2100 under the SSPs. They offer projected urbanization levels every five years for 204 countries and areas, and annual projections from 2010 to 2100 for 188 countries and areas using historical data from the World Bank. He et al. (2023) developed a global dataset of urban fractional changes at 1 km resolution from 2020 to 2100 under eight SSP-RCP (Representative Concentration Pathways) scenarios. Their approach involves characterizing impervious surface area (ISA) growth patterns using a sigmoid model, integrating these patterns with a CA model, and calibrating state-specific urban CA models for projections based on Land Use Harmonization2 (LUH2) data. Varquez et al. (2017) calibrated a SLEUTH urban growth model for Jakarta's 2050 expansion, incorporating SSPs, population projections, and empirical relationships between population, nighttime lights, urban parameters, and GDP. They emphasized the importance of the Spread and Breed coefficients in the SLEUTH model, as they affect the growth speeds and modified these coefficients by optimizing them with the Monte Carlo simulation of SLEUTH to match the urbanization trend.

1.3 RCP framework for flood risk assessment

The RCPs describe different greenhouse gas concentration trajectories and project climate change impacts up to 2100 (Taylor et al. 2012). They are based on socioeconomic emission assumptions and have been adopted by the Intergovernmental Panel on Climate Change (IPCC) (van Vuuren et al. 2011). RCPs serve as inputs for Global Climate Models (GCMs), such as those used in the Coupled Model Intercomparison Projects (CMIPs), and Regional Climate Models (RCMs) to simulate future climate conditions, including changes in temperature, precipitation, and sea level rise (Eyring et al. 2016). In CMIP6 (IPCC Sixth Assessment Report), RCPs are integrated with SSPs to provide a more comprehensive assessment of socioeconomic changes and climatic effects (O'Neill et al. 2016).

These climatic factors directly influence flood risk by altering rainfall intensity, river discharge, and coastal storm surges. Hydrological models use RCP-driven climate projections to estimate changes in river runoff, soil moisture, and groundwater levels (Wang et al. 2024). These outputs are then used by hydraulic and hydrodynamic models to simulate water movement through river networks, floodplains, and urban environments (Schumann et al. 2018; Kumar et al. 2023).

1.4 Study objectives and approach

Balancing the complexity of urbanization dynamics with diverse socioeconomic narratives and bringing them together with climatic scenarios necessitates an innovative approach. In response, this paper investigates the predictive capabilities of the SLEUTH model using

future-oriented SSP- and RCP-based scenarios and examines their thematic outcomes.

While previous studies mostly focus on single-city analyses or consider socioeconomic and climatic drivers in isolation, there is a lack of integrated, multi-scenario, and multi-study area assessments that combine SSP-RCP frameworks with spatially explicit urban growth and flood exposure modelling. Furthermore, scaling urban models to larger, heterogeneous areas requires methodological adaptations, such as spatial tiling and distinguishing between urban and rural growth characteristics, both underexplored in earlier research.

To address these gaps, this exploratory research applies a harmonized scenario framework to nine coastal cities across three continents in the Global South for urban growth modelling and flood exposure assessment. The focus on the Global South is particularly relevant, as these regions are experiencing some of the world's fastest urbanization rates (Randolph and Storper 2022). The study areas were selected for their diverse geographic, climatic and environmental contexts, as well as previous flood experience. This diversity is crucial for understanding how different regions with unique characteristics respond to urbanization and climate change, highlighting urban growth hotspots in coastal, fluvial and pluvial flood regimes. Additionally, understanding urban growth dynamics and their implications for flood risk in the Global South is critical for sustainable development and resilience building (Sett et al. 2024), with lessons that can inform policies and strategies in similar contexts globally (Pirani et al. 2024).

This study evaluates whether SSP- and RCP-based scenarios can be effectively integrated into a SLEUTH-based urban growth modelling approach through the model-inherent Breed and Spread coefficients and applied in subsequent flood exposure analysis to simulate plausible future urban expansion and associated flood risks.

The study is guided by the following key research questions:

- How will future urban growth under different SSP-RCP scenario combinations affect exposure to coastal, fluvial, and pluvial flooding in rapidly urbanizing cities of the Global South?
- How do urbanization patterns and flood exposure trends differ across these diverse settings, and what commonalities emerge from a cross-continental comparative analysis?

Additionally, the study design enables us to draw conclusions about how urban growth modelling approaches can be further adapted for consistent, high-resolution application across large and heterogeneous study areas. The year 2050 was chosen as a mid-century benchmark that aligns with global policy targets (UNFCCC 2015) and offers more reliable projections than longer-term horizons. This timeframe provides actionable insights for urban planning and flood risk mitigation in rapidly growing cities. By producing scenario-based, spatially explicit insights at 30 m spatial resolution, this study addresses the challenges and opportunities presented by urbanization, climate change, and flood exposure, offering insights into current conditions and future scenarios for risk informed decision-making and resilience building.

2 Data and methodological approach

2.1 Study areas

For this study, the selection of coastal cities aimed to represent a broad distribution across global ocean coasts while including only cities in the Global South. We selected nine coastal or coastal-zone agglomerations in the Global South based on the following criteria:

1) They already have a large population of at least 2 million inhabitants.
2) They are recognized as rapidly growing/dynamically changing cities.
3) They experienced flood events in the past.
4) They are situated along coastlines, river courses, and/or are affected by tidal activity, exposing them to both sea-level rise and riverine flooding due to climate change in the future.

Hanson et al. (2010) ranked coastal and port cities by climate extremes, identifying five cities (Lagos, Khulna, Abidjan, Surat and Ho Chi Minh City) from our selection among the top 20 with the "highest proportional increase in exposed population by the 2070s". Nicholls and Cazenave (2010) noted that most Asian countries face sea-level rise (SLR) threats due to densely populated river deltas with large, fast-growing cities. Similarly, Africa's coasts are at risk due to lower levels of development and assumed rapid population growth (Dasgupta et al. 2010). Our study, along others (Nicholls et al. 2008; Nicholls and Cazenave 2010; Rosenzweig et al. 2018), lists cities at risk in coastal Asia and Africa. Additionally, we included two South American cities identified in climate reports and scientific publications (World Bank 2014; Reguero et al. 2015) as being at significant risk.

Each study area encompasses not only the administrative area of the city but also the periurban region and surrounding settlements, including satellite cities, towns, villages, and rural lands, forming a larger urban agglomeration. The administrative units analysed for each city and further details about population, past growth and historic flood events can be found with Supplementary

Table 1. Throughout the following text, city names represent their entire agglomeration.

Among the selected agglomerations, Abidjan, Lagos, and Dar es Salaam are among Africa's largest and fastest-growing coastal cities (Fig. 1). Abidjan and Lagos situated along the Atlantic Ocean, are bordered by lagoons fed by inland tributaries. Abidjan is the largest city in the Ivory Coast and has faced multiple severe pluvial and river flooding events in recent years. Lagos is affected mainly by pluvial floods, but compound flood is an increasing threat (Nkwunonwo et al. 2016). Dar es Salaam, Tanzania's largest city and located at the Indian Ocean, is vulnerable to coastal, pluvial, and compound fluvial-pluvial floods (Kebede and Nicholls 2011).

Ho Chi Minh City, Vietnam's largest city, lies downstream of the Dong Nai and Saigon Rivers (Fig. 2). It experiences flooding caused by extreme monsoon rainfall and tidal events (Couasnon et al. 2022). Khulna, Bangladesh, is positioned within the Sundarbans/Brahmaputra–Meghna Delta. Even though the city is approximately 100 km from the Bay of Bengal in the Indian Ocean, its deltaic and low-lying topography makes the region exposed to pluvial and fluvial, but also cyclonic coastal flooding (Haque and Nicholls 2018; Bernard et al. 2022). Surabaya, the capital of East Java Province in Indonesia, lies on the low-lying northern coast of Java, where several river arms make it prone to river and tidal flooding (Susetyo et al. 2022). Surat, in Gujarat, India, is one of the world's fastest growing cities, positioned along the Indian Ocean and Tapi River. Since a devastating flood in 2006, it has faced frequent coastal, fluvial and pluvial flood events, particularly during the monsoon season (Jamshed et al. 2023; Jibhakate et al. 2023).

Barranquilla, Colombia's largest coastal city and the capital of the Atlántico Department, is located at the delta of the Rio Magdalena, where it meets the coast of the Caribbean Sea and faces multiple flood hazards (Fig. 3) (Milanes et al. 2021). Guayaquil, the largest city in Ecuador, lies where the Babahoyo River and Daule River merge into the Guayas River, forming Latin America's largest delta before draining into the Pacific (Pelckmans et al. 2023). Our analysis included Guayaquil (excluding Isla Puna and the enclave of Tenguel), along with eight neighbouring cantons. In early 2023, the study area suffered from severe pluvial and river flooding (IFRC 2023).

2.2 Data

2.2.1 Flood hazard layers

Global flood hazard layers for a variety of scenarios are available from the Fathom Global Flood Map 3 (Fathom 2023). The flood modelling is based on the FABDEM+ digital elevation model (DEM) with a 30 m spatial resolution (Hawker et al. 2022). The FABDEM is a global ground terrain map, derived from the Copernicus DEM (Airbus 2019), in which tree canopies and building roofs have been removed. FABDEM+ is a composite of FABDEM (Hawker et al. 2022) and publicly available LiDAR data. The Fathom flood model applies a hydraulic model

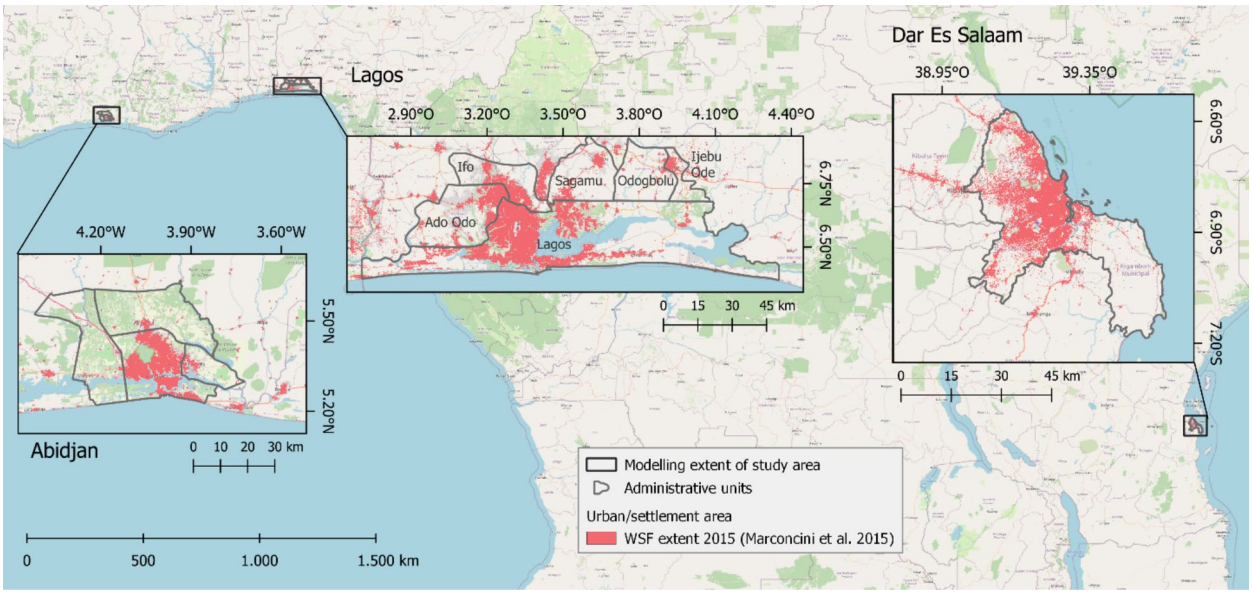

Fig. 1 Agglomerations of Abidjan, Lagos and Dar es Salaam in Africa. The modelling was conducted for the rectangular areas, while further analysis is based on administrative units. Administrative boundaries and the base map are provided by OpenStreetMap and the OpenStreetMap-Foundation (CC-BY-SA)

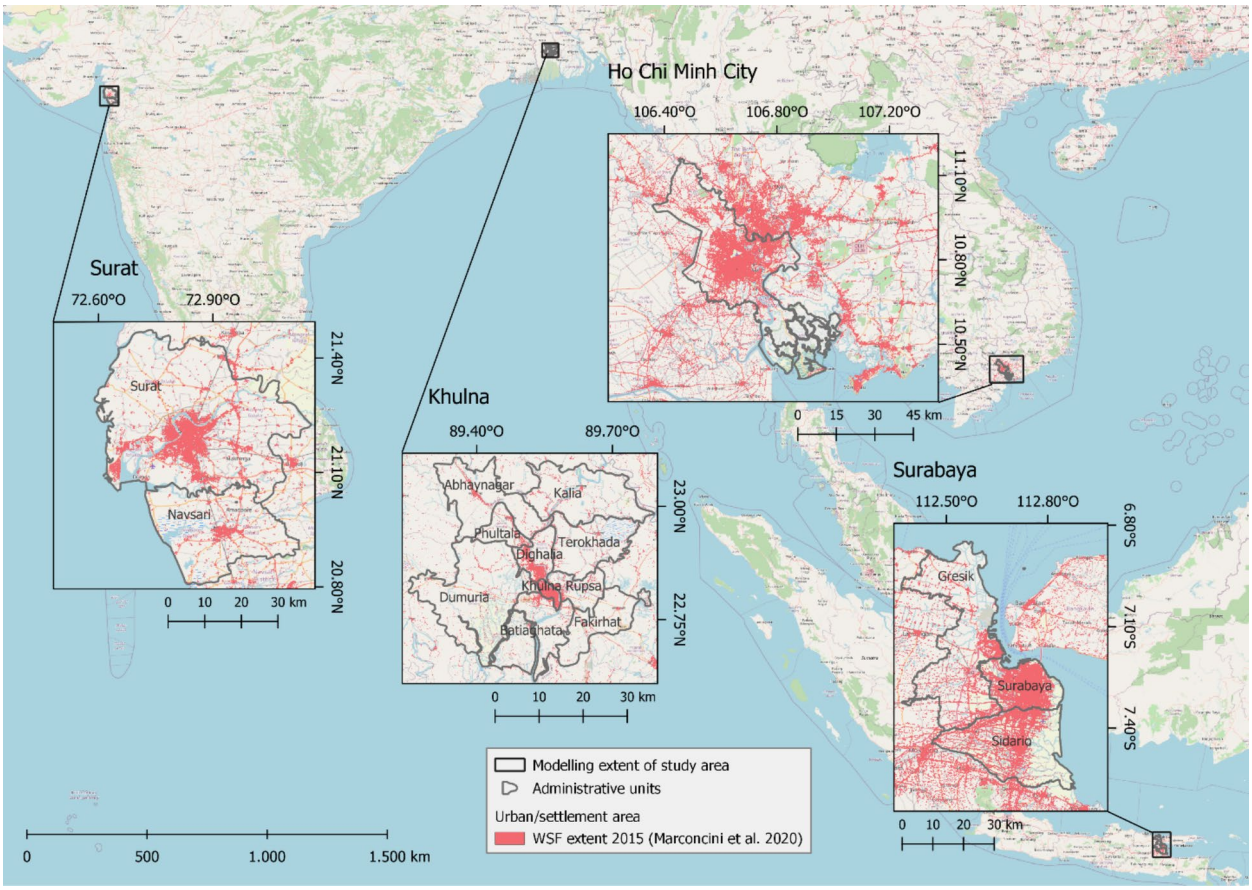

Fig. 2 Agglomerations of Surat, Khulna, Surabaya and Ho Chi Minh City in Asia. The modelling was conducted for the rectangular areas, while further analysis is based on administrative units. Administrative boundaries and the base map are provided by OpenStreetMap and the OpenStreetMap-Foundation (CC-BY-SA)

to produce flood hazard maps, based on the inertial formulation of the shallow water equations, adapted for two-dimensional inundation modelling by Bates (2022). The size of rivers is simulated using a gradually-varied flow solver (Neal et al. 2021). Further information about the Fathom Global 3.0 methodology can be found in Fathom (2022a, b).

The Global Flood Map data comprise inundation depths and risk scores for inland flooding (pluvial and fluvial) and coastal flooding at a 30 m spatial resolution (Fathom 2023). The flood data are generated for a set of associated climate dynamics, allowing for flood maps to be derived under different projected climate conditions. Future scenarios can be derived selecting year and climate projection (based on different climate scenarios or global mean temperature changes) (Fathom 2023). Additionally, percentile-based flood depth data represent climate model uncertainty, with the range between the 17th and 83rd percentiles aligning with the IPCC definition of 'likely' (Fathom 2023), with the 50th percentile representing the median, meaning half the simulations show lower magnitudes and half show higher. For this study, we retrieved Global Flood Map 3 data for the selected study areas with the specifications: Year: 2050; Scenarios: RCP2.6, RCP4.5, RCP8.5; Percentiles: 50th, 83rd; Metric: depth; Flood types: pluvial/fluvial/coastal; Return period: 100-years.

For fluvial and coastal flood scenarios, the dataset allows the selection of defended and undefended local conditions. In this study, we intentionally decided for the defended status, wherein known flood defences are incorporated and thereby best representing the local situation best (see Fathom (2022a, b)).

2.2.2 World settlement footprint evolution

The World Settlement Footprint (WSF)-evolution dataset is an open-access information product that maps the urbanization process at a global scale (Marconcini et al. 2020). The WSF-evolution dataset is generated using Sentinel and Landsat data and delineates the global settlement extent through annual binary images at a 30 m resolution for the years 1985

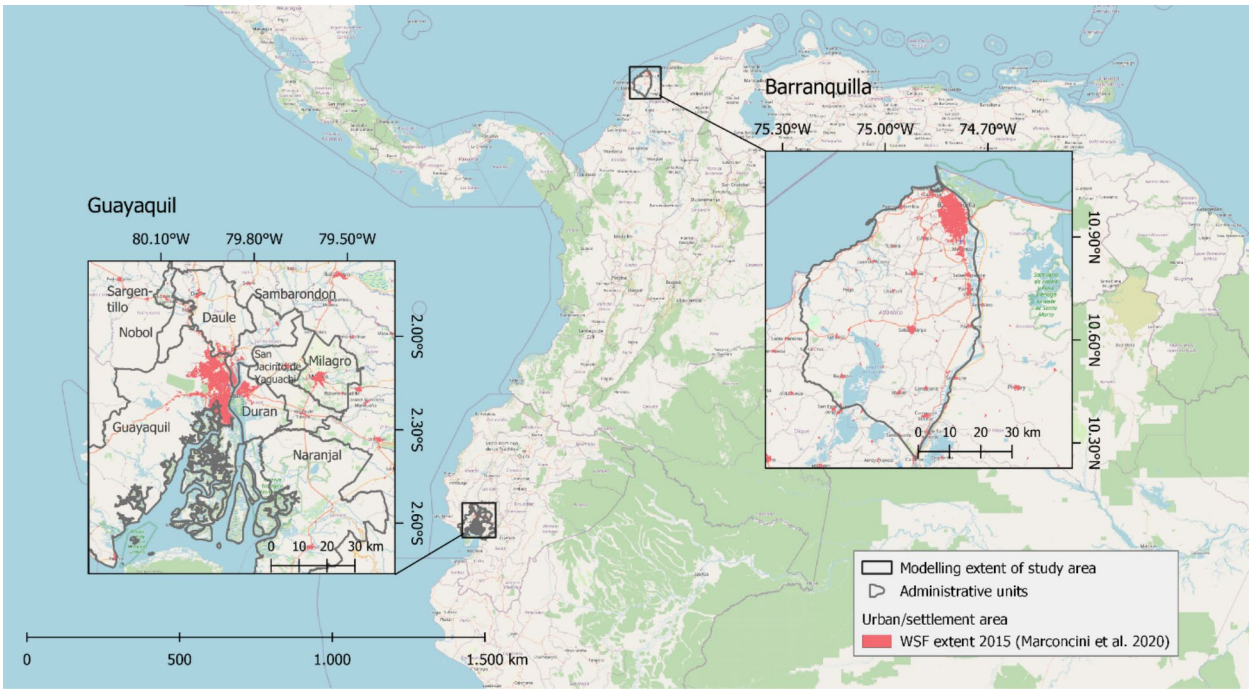

Fig. 3 Agglomerations of Guayaquil and Barranquilla in South America. The modelling was conducted for the rectangular areas, while further analysis is based on administrative units. Administrative boundaries and the base map are provided by OpenStreetMap and the OpenStreetMap-Foundation (CC-BY-SA)

to 2015. The WSF was selected for this study because its consistent annual binary classification of settlement (comprising built-up structures and impervious intra-urban surfaces) and non-settlement areas over an extended time period makes it particularly well-suited as an input for the SLEUTH model. In this study, the WSF-evolution was used to generate historical urban extent layers for the calibration and prediction of the SLEUTH model.

2.3 SSP-RCP scenario integration

This study integrates socioeconomic scenarios from the SSPs database (IIASA 2018) to predict future urban growth. O'Neill et al. (2016) applied these SSPs within the Scenario Model Intercomparison Project (ScenarioMIP) to assess combinations of SSPs and RCPs. From the IPCC's RCP scenarios (van Vuuren et al. 2011, 2013), we selected three to represent a broad range of possible futures: low forcing (RCP2.6), medium stabilization (RCP4.5), and high emission (RCP8.5). Correspondingly, we focused on three Tier 1 scenarios, combining SSPs and RCPs based on their plausibility and concurrent occurrence: SSP1/RCP2.6, SSP2/RCP4.5 and SSP5/RCP8.5 (see Table 1).

2.4 Urban growth modelling

2.4.1 SLEUTH model

The SLEUTH model is a CA-based framework for simulating urban expansion and land use changes (Clarke et al. 1997, Clarke et al. 2004). It assumes that urbanization underlies development patterns distinctive to an urban agglomeration and observable in the historical development. The SLEUTH model relies on five control parameters that describe different urban growth patterns:

- Spread coefficient: Governs the contagious influence of established urban areas on their surroundings, impacting the spatial patterns of urban growth.
- Breed coefficient: Represents the probability that a newly formed detached settlement will initiate its independent growth cycle.
- Diffusion: Governs the random selection frequency of a pixel for potential urbanization.
- Slope resistance: Acknowledges the topographical constraints, ensuring that the model considers the resistance posed by elevated terrains to urban expansion.
- Road gravity factor: Serves as an attraction force, drawing new settlements towards existing roads and guiding the expansion along road networks.

Table 1 Short description of SSP scenarios, RCP scenarios and Tier 1 scenarios of the ScenarioMIP investigated in this study

SSP Scenarios	2100 Forcing Level (W m^2)	SSP-RCP
SSP1 – Sustainability: A future world where countries develop sustainably. High-income countries support low-income countries, and international cooperation and technology advancements accelerate. Fossil fuel reliance decreases, and there is a redistribution of resources. Compact, high-quality cities with complete infrastructures experience rapid urbanization worldwide (van Vuuren et al. 2017)	RCP2.6: This scenario embodies a proactive approach to mitigation, where the radiative forcing level is significantly curtailed. It envisions a concerted global effort to reduce greenhouse gas emissions, resulting in substantial progress toward averting severe climate change	SSP1/RCP2.6: This scenario paints a future world marked by advanced technology and sustainable development. Thanks to remarkable technological strides, urban centres are poised for rapid expansion, resulting in a substantial increase in urban populations. Simultaneously, rigorous emission controls ensure that the world successfully maintains low emission levels, leading to a notable deceleration of climate change
SSP2 – Middle of the Road: A future development scenario aligned with historical trends. Some international cooperation exists, and energy/resource intensity slightly decreases. Fossil fuel consumption remains significant, and cities in all countries develop at a moderate pace. The SSP2-middle of the road can be referred to as business as usual (BaU) (Fricko et al. 2017)	RCP4.5: Positioned as an intermediate radiative forcing level, this scenario anticipates emissions peaking around the year 2040, followed by a gradual decline. It reflects a world where emissions are mitigated but not as drastically as in RCP2.6	SSP2/RCP4.5: This scenario portrays a world characterized by intermediate emission levels, where cities evolve in harmony with historical development trends. It reflects a path of gradual but not radical mitigation efforts
SSP5 – Fossil-Fueled Development: Economic growth drives social and economic development, resulting in high energy demands and continued dominance of fossil fuels. Environmental degradation occurs globally, and rapid population growth leads to an accelerated urbanization process worldwide (Kriegler et al. 2017)	RCP8.5: As the high radiative forcing level baseline, this scenario envisions emissions persisting and even increasing throughout the twenty-first century. It serves as a sobering portrayal of a future where fossil fuels continue to dominate the energy landscape, exacerbating climate change consequences	SSP5/RCP8.5: This scenario envisions a future heavily reliant on fossil energy as the primary energy source. In this trajectory, cities experience unbridled growth, unhampered by emission limitations. However, the perilous consequence is accelerated climate change, resulting in a heightened frequency of flood hazards

Based on the control parameters, the behaviour of four key growth rules is adjusted (Clarke et al. 2004):

- Spontaneous Growth: This encompasses the random urbanization of cells or pixels, influenced by diffusion and slope resistance.
- New Spreading Center Growth: Often referred to as diffusion growth. This aspect governs whether a pixel or a cluster of pixels evolves into a new urban centre and is influenced by breed and slope resistance.
- Edge Growth: Termed organic growth, representing urban expansion at the fringes of existing urban centres. This growth behaviour is influenced by spread and slope resistance.
- Road-Influence Growth: This mechanism accounts for urban development along road networks or transportation corridors. This aspect is influenced by breed, road gravity, diffusion and slope gravity.

In addition, the modelling approach allows the exclusion of specific areas that are kept free from future urban development due to different reasons, such as national parks or places of religious importance.

2.4.2 Zoning and tiling of the study areas

Urban regions often exhibit varying development speeds across different zones, particularly when the administrative planning area encompasses both urban and rural domains. However, the SLEUTH model applies a single set of coefficients for the entire study area, leading to uniform urban growth patterns that do not account for local differences in urbanization dynamics. To address this, we introduced a zonation approach using kernel density estimation (KDE) and k-means clustering (Silverman 1986).

For the KDE calculation, a circular kernel size of 100 pixels was chosen. The resulting kernel image was then classified using k-means clustering, differentiating between urban and rural-dominated areas. Each city was divided into five clusters, representing different urbanization levels (I-V). Clusters I and II exhibited urban characteristics, while levels III, IV, and V were categorized as "rural" (Fig. 4). Notably, these classifications do not reflect functional urban–rural distinctions, but rather denote zones with distinct growth rates and spatial patterns.

To enhance local calibration, SLEUTH coefficients were adjusted separately for urban and rural zones. To improve computational efficiency, rural zones were further divided into 4 to 9 tiles, depending on the size of the study area. In the case of Lagos, the urban zone was also divided into two tiles to allow for more precise calibration. In total, tiling and zonation resulted in 95 tiles across the 9 cities. The impact of this zonation approach was evaluated using the Area Under the Curve (AUC) metric to assess prediction accuracy.

2.4.3 SLEUTH calibration, evaluation and prediction

The SLEUTH model implementation consists of two phases: 1) calibration and evaluation, and 2) the prediction of urban growth, which is conducted individually for all 95 obtained tiles (Fig. 5). For calibration, the 1985 urban and settlement extent layers were set as seed layers, while the layers 1990, 1995, 2000, 2005, and 2010 served as reference data. The input data used to determine the SLEUTH parameters for each city are listed in Table 2.

The optimal coefficient combination was determined through a three-step 'brute-force calibration' process (coarse, fine, and final) (Clarke et al. 1996). Instead of this original grid-search method, we employed a genetic algorithm-based SLEUTH model to project future urban expansion based on Clarke (2018). In the genetic algorithm (GA) calibration process, an initial parameter set is

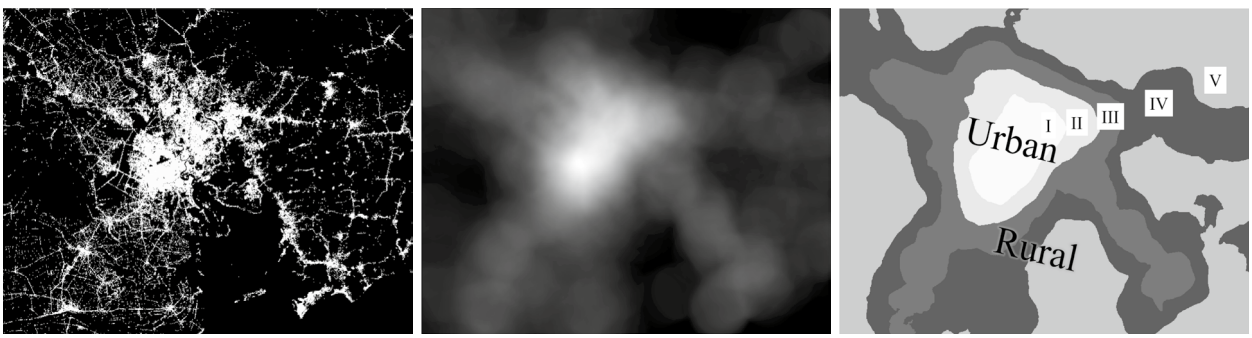

Fig. 4 Zonation approach using Kernel Density Estimation (KDE) for Ho Chi Minh City (HCM)**. a** WSF-evolution (2015) depicting urban extent; (**b**) Kernel density image derived from WSF-evolution; (**c**) Zonation classification using k-means clustering**,** with Levels **I–V** representing different settlement density zones

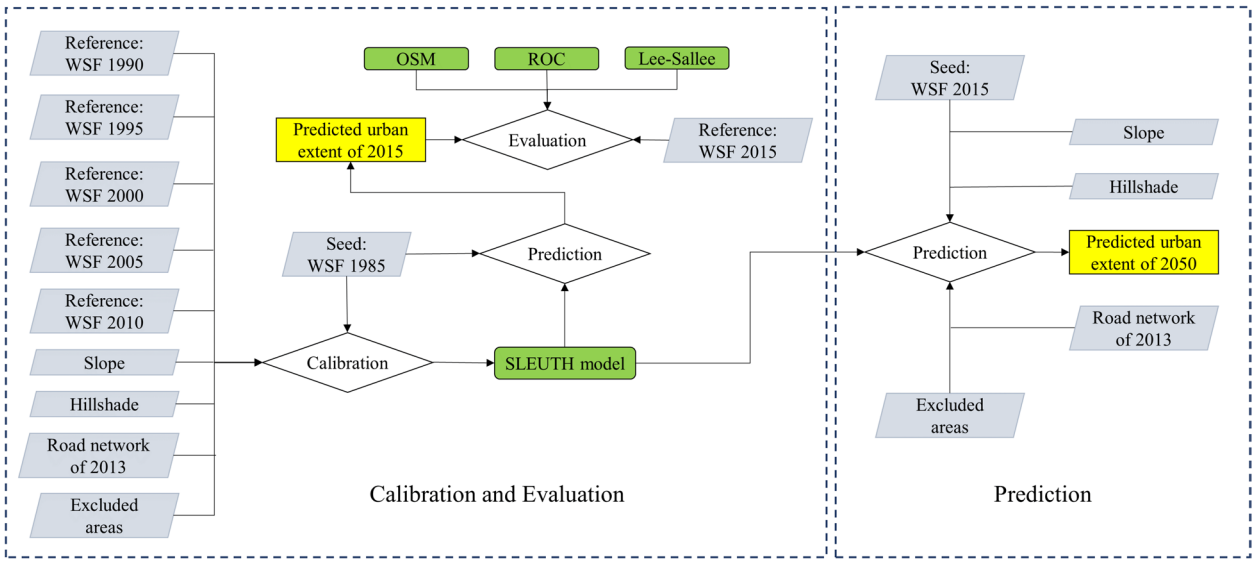

Fig. 5 SLEUTH model implementation – Calibration and evaluation process (left) and prediction workflow (right)

Table 2 Input layers for SLEUTH model calibration

Layer Name	Variables	Year	Spatial Resolution	Source/Reference
WSF-evolution	Historical settlement extent layers	1985–2015	30 m	WSF-evolution (Marconcini et al. 2020)
Global Roads Open Access Data Set (gROADs)	Traffic networks	2013	-	gROADS v1. (Center for International Earth Science Information Network CIESIN et al. 2013)
Copernicus DEM	Slope and hillshade	-	30 m	Copernicus DEM (European Space Agency and Airbus 2022)
Sentinel-1/Sentinel-2	Water mask	2020	30 m	Copernicus Sentinel data 2020)
The World Database on Protected Areas (WDPA)	Areas excluded from settlement development	Download version August 2022	-	The World Database on Protected Areas (UNEP-WCMC and IUCN 2023)

iteratively mutated and refined, with poorly performing combinations replaced by new ones based on their performance metrics. This approach yields results comparable to the brute force method while significantly reducing computation time.

To assess calibration quality and improve prediction accuracy, we applied the Optimal SLEUTH Metrics (OSM) (Dietzel and Clarke 2007; Kumar and Agrawal 2022). OSM serves as a composite performance measure in the SLEUTH model calibration process. It is derived from the product of seven SLEUTH inherent fit metrics for calibration: compare, population, edges, clusters, slope, X-mean, and Y-mean. These metrics collectively evaluate how well the simulated urban growth aligns with observed historical patterns in terms of spatial accuracy and structural characteristics (Dietzel and Clarke 2007).

Beyond OSM, we applied the Lee-Sallee index (Lee and Sallee 1970) and Receiver Operating Characteristic (ROC) curve, evaluated using the AUC (Hanley and McNeil 1982; Park et al. 2004), to assess predicted urban/settlement growth until 2015 against the WSF reference dataset. The Lee-Sallee index measures shape similarity between predictions and reference data. However, when combined with other indices, it offers valuable performance insights. Saxena and Jat (2020) compared various publications and found that a value of 0.3 (1.0 being a perfect match) is acceptable, with some models achieving values above 0.6 (Jantz et al. 2016; Harb et al. 2020). The AUC metric assesses overall model accuracy, illustrating the relationship between true-positive false-positive rates across different classification thresholds (Pontius and Schneider 2001; Wu et al. 2008). An AUC of 1 indicates perfect predictions, while 0.5 suggests random guessing. Typically, an AUC above 0.75 is considered good (Verburg et al. 2004). Combining these indices provides a robust

framework for evaluating urban growth models from multiple perspectives.

For predicting the 2050 settlement extents, the 2015 urban and settlement extent layers were used as seed layers, along with the parameter sets derived from calibration (including adjusted Spread and Breed coefficients) and additional input layers (Fig. 5, right).

2.4.4 Integration of SSPs into the SLEUTH model

The SSP Database (IIASA 2018) provides long-term socioeconomic projections (population, urbanization, and GDP) up to 2100, enabling urban growth analysis under different development trajectories (Riahi et al. 2017; IIASA 2018). In this study, we focus on SSP1, SSP2 and SSP5, which are associated with RCP scenarios 2.6, 4.5 and 8.5, respectively, to cover a full range of future challenges to climate mitigation from low (SSP1), to medium (SSP2), to high (SSP5) (O'Neill et al. 2016). The SSP database provides national and regional urbanization projections at 5-year intervals. For our study, we used the national projections from 2015 and 2050 (Jiang and O'Neill 2017) and calculated relative trends in urban population share and population numbers projected by the SSPs (compare with Supplementary Figs. 1 and 2). We translated the relative growth of the urban population into spatial expansion patterns, following the assumption that urbanization is linearly related to increases in the urban population. To represent the SSP scenarios in the simulations, the Breed and Spread coefficients of the SLEUTH model were adjusted to reflect different growth speeds and patterns in SSP1, SSP2, and SSP5. First, the set of coefficients for each city, calibrated from historical growth, was kept constant, serving as the baseline for SSP2 – also known as the Business as Usual (BaU) scenario. For SSP1 and SSP5, the Spread and Breed coefficients were modified based on their relative differences from the SSP2 baseline, following Eqs. (1) and (2):

$$\Delta UP_t = US_{2050,t} \bullet Pop_{2050,t} - US_{2015,t} \bullet Pop_{2015,t} \tag{1}$$

$$\frac{S_t, B_t}{S_{SSP2}, B_{SSP2}} = \frac{\Delta UP_t}{\Delta UP_{SSP2}} \tag{2}$$

where ΔUP represents the change in total urban population, while *US* denotes the urban share and *Pop* the population number for each SSP scenario *t*. *S* and *B* correspond to the Spread and Breed coefficients, respectively. In this way, the relative differences in growth rates between SSP1 and SSP5, compared to SSP2, are effectively captured.

2.4.5 Future flood exposure analysis

The projected urban and settlement growth under the three SSP scenarios were overlaid with Fathom flood layers to assess the potential flood exposure in 2050. For coastal, fluvial and pluvial flooding, we selected the 50th and 83rd percentile flood layers. The analysis separately examined:

- The total urban areas at flood exposure risk in 2050, and
- New urban/settlement areas projected to be at flood exposure risk by 2050.

The workflow of the flood exposure estimation is illustrated in Fig. 6. Following Wing et al. (2017) and Tate et al. (2021), flood pixels with depths below 15 cm were excluded, as such shallow flooding is generally below the

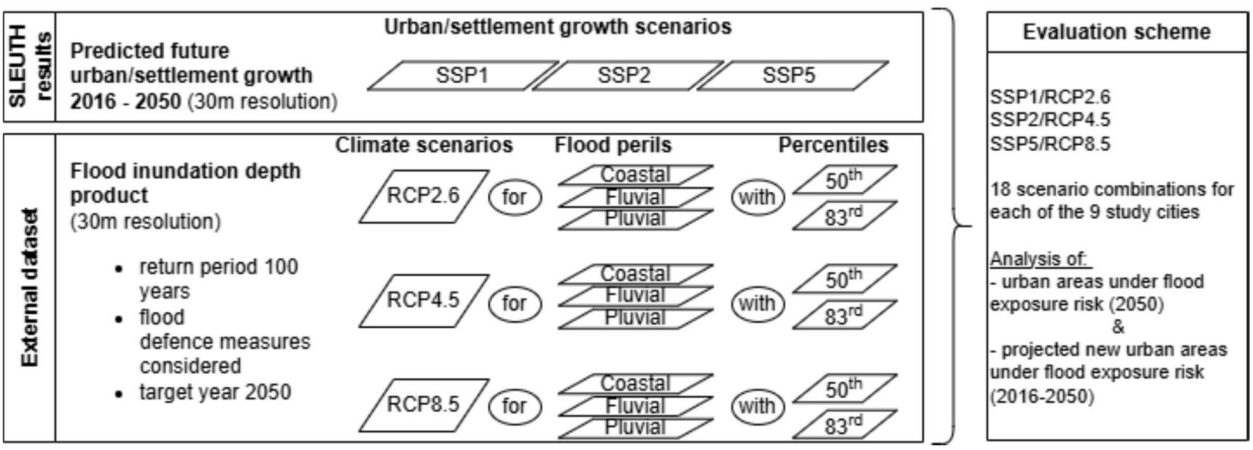

Fig. 6 Workflow of future flood exposure risk analysis. Urban and settlement growth projections for 2050 (based on SSP scenarios) are overlaid with flood inundation data for RCP2.6, RCP 4.5 and RCP8.5 climate scenarios. The analysis considers coastal, fluvial and pluvial flooding with the 50th and 83rd percentile flood depth estimates

threshold for significant damage. Only areas with flood depths exceeding 15 cm were considered as ground flood plains under exposure.

3 Results

3.1 SLEUTH calibration based on KDE zonation

The SLEUTH model was successfully configured for the nine coastal agglomerations, capturing the gradients in growth speeds and patterns for urban and rural zones. To evaluate the KDE-based zonation approach, SLEUTH-predicted urban growth (1985–2015) with and without zonation for Surat and Surabaya was compared with the 2015 WSF extent. AUC values confirmed improved accuracy with zonation (Table 3). These two cities were selected as representative case studies to evaluate the added value of KDE-based zonation in detail, while the approach was applied uniformly across all study areas to support locally calibrated urban growth projections. Consequently, this approach was adopted throughout the study.

Model accuracy was assessed using the Lee-Sallee index and AUC, while OSM was primarily used to fine-tune SLEUTH parameters. Both AUC and Lee-Sallee index demonstrated notable modelling accuracies, with values ranging from 0.73 to 0.94 and 0.56 to 0.82, respectively. The AUC consistently indicated high predictive performance across all cities, with Khulna nearing the 0.75 threshold, signifying a good predictive outcome (Verburg et al. 2004). Meanwhile, the Lee-Sallee index highlighted significant shape similarities, aligning with findings from previous studies (Saxena and Jat 2020). For a detailed breakdown of the evaluation results, refer to Fig. 7. Contrary to the default setting, the Critical-Low threshold that controls the self-modification component of the SLEUTH model was reduced from 0.95 to 0.7. This adjustment improved the model performance by better reflecting the differing development patterns of neighboring tiles (see Clarke et al. 1997). In a few exceptions, the value was further lowered after visual control to minimize outlier tiles and to ensure more consistent growth across the tiles of the city.

3.2 Prediction of urban/settlement growth in SLEUTH

During calibration, the Breed and Spread coefficients of SSP2 for each city were generated from the WSF data. The coefficients for SSP1 and SSP5 were computed using Eqs. (1) and (2). The resulting relative changes in the SSP scenarios, along with the adjusted SLEUTH parameters, are listed in Supplementary Tables 2 and 3.

The predicted urban growth (2016–2050) under different SSPs was generated based on the coefficient sets, with diffusion, road gravity, and slope resistance remaining constant under all the scenarios. Figure 8 illustrates urban/settlement growth for SSP2, while results for SSP1 and SSP5 are presented in the Supplement (Fig. 3 and 4). All study areas face significant increases in urbanized area throughout the three scenarios, however with different growth dynamics. Urbanization patterns in Abidjan, Barranquilla and Dar es Salam are mainly characterized by compact growth, whereas urban sprawl dominates in Ho Chi Minh City, Khulna and Surat.

Figure 9 presents a quantitative overview of future urban growth areas and growth rates for select cities. This visualization highlights four cities experiencing growth exceeding 50% under SSP1/SSP5: Surat, Khulna, Ho Chi Minh City in SSP1 and SSP 5, and Dar es Salaam. Among them, Khulna exhibits the highest growth, reaching 196.9% in SSP2 and surging to 210.8% in SSP1. In contrast, Abidjan, Surabaya (in SSP2) and Lagos show relatively lower growth rates compared to other agglomerations with less than 25% of urban growth.

Table 3 Evaluation of the KDE-based zonation method using AUC values from the predicted urban probability maps

City	Without zonation	With zonation
Surat	0.83	0.85
Surabaya	0.84	0.87

3.3 Future flood exposure analysis

3.3.1 Coastal flood exposure

The anticipated coastal flood plains until 2050 under the SSP2/RCP4.5 scenario are exemplarily illustrated in Fig. 10, alongside the projected urban extents of the agglomerations. This provides insight into potential flood-prone areas and their interactions with future urban expansion. The results highlight varying impacts on urban and settlement areas, with Khulna notably experiencing no impact from exclusive coastal flooding. For Abidjan, Barranquilla, Ho Chi Minh City, and Guayaquil, flood-exposed areas remain minimal (< 1 km^2 across all scenarios), while Surabaya faces the most severe impacts, with 74 km^2 (SSP1/RCP2.6, 83rd percentile), 68 km^2 (SSP2/RCP4.5), and 83 km^2 (SSP5/RCP8.5) affected (Fig. 11).

Future coastal flood exposure remains stable in Abidjan, Barranquilla, and Guayaquil, but Dar es Salaam, Surabaya, and Surat are projected to experience the highest absolute increases in flood-prone areas, with additional extents of 4.18 km^2, 16.52 km^2, and 5.09 km^2 (50th percentile) under SSP5/RCP8.5. Among cities with significant inundation, such as Surat, Surabaya, and Lagos, the SSP5/RCP8.5 scenario consistently projects the highest flood exposure. In contrast, the SSP2/RCP4.5 "Middle of the Road" scenario yields the lowest exposure, except

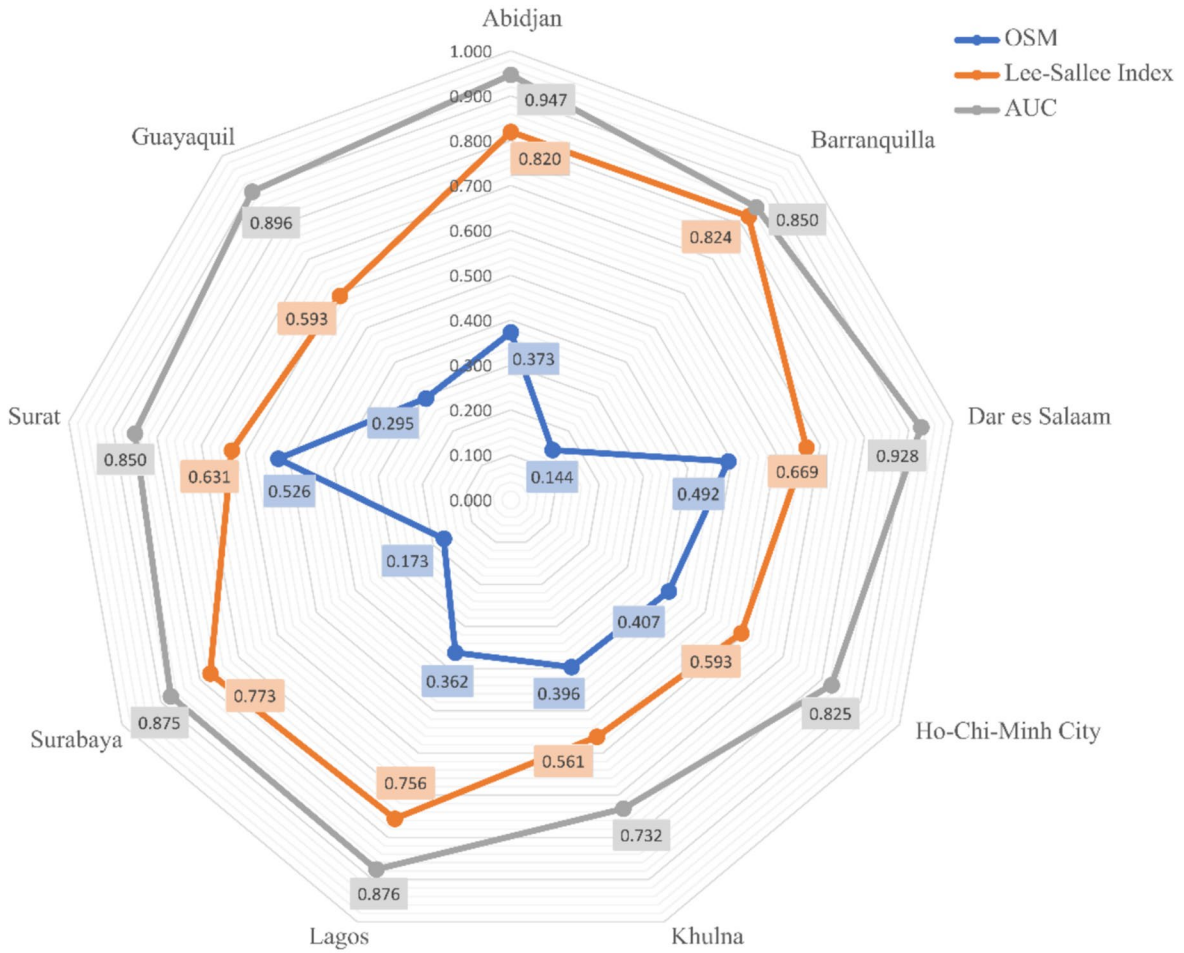

Fig. 7 Accuracy assessment results based on OSM, Lee-Sallee Index, and AUC, illustrating model performance across all cities

in Lagos, where SSP1/RCP2.6 predicts the least inundation (Supplementary Table 4).

3.3.2 Riverine flood exposure

The floodplains of the study agglomerations projected for 2050 under SSP2/RCP4.5 are illustrated in Fig. 12, with different shades of blue indicating varying inundation depths. Fluvial flood patterns are strongly influenced by local topography and hydrology, with Surabaya and Ho Chi Minh City facing the highest future exposure. For the 83rd percentile, Surabaya's urban area could potentially experience 200 km^2 of flooding, while Ho Chi Minh City could experience 150 km^2 of flooding. In Guayaquil, over 18–25% of the total 2050 urban area may be affected by riverine flooding under all scenarios, with the cantons of Daule, Samborondón, San Jacinto de Yaguachi, and Durán being particularly vulnerable. Barranquilla exhibits the highest inundation depths (> 3 m) in urban areas.

Figure 13 shows the extent of riverine flooding for each city under SSP1/RCP2.6, SSP2/RCP4.5, and SSP5/RCP8.5 (see Supplementary Table 5 for detailed projections). The results reveal stark disparities in exposure trends. Guayaquil emerges as a critical case, with over 37% of newly developed built-up areas projected to be flood-exposed by 2050; nearly double the 2015 baseline (Table 4). Similarly, Ho Chi Minh City is expected to see over 20% of its new urban zones affected. In contrast, Abidjan, Barranquilla, and Lagos exhibit relatively low exposure, with built-up areas facing minimal increases (e.g., Abidjan: < 0.46 km^2 for the 50th percentile). However, Dar es Salaam and Khulna show more than a doubling of flood exposure under all scenarios, underscoring the compounding risks of rapid urbanization and fluvial flooding. Notably, newly developed areas in Abidjan and Dar es Salaam face disproportionately higher exposure compared to existing urban zones, despite their overall lower flood magnitudes.

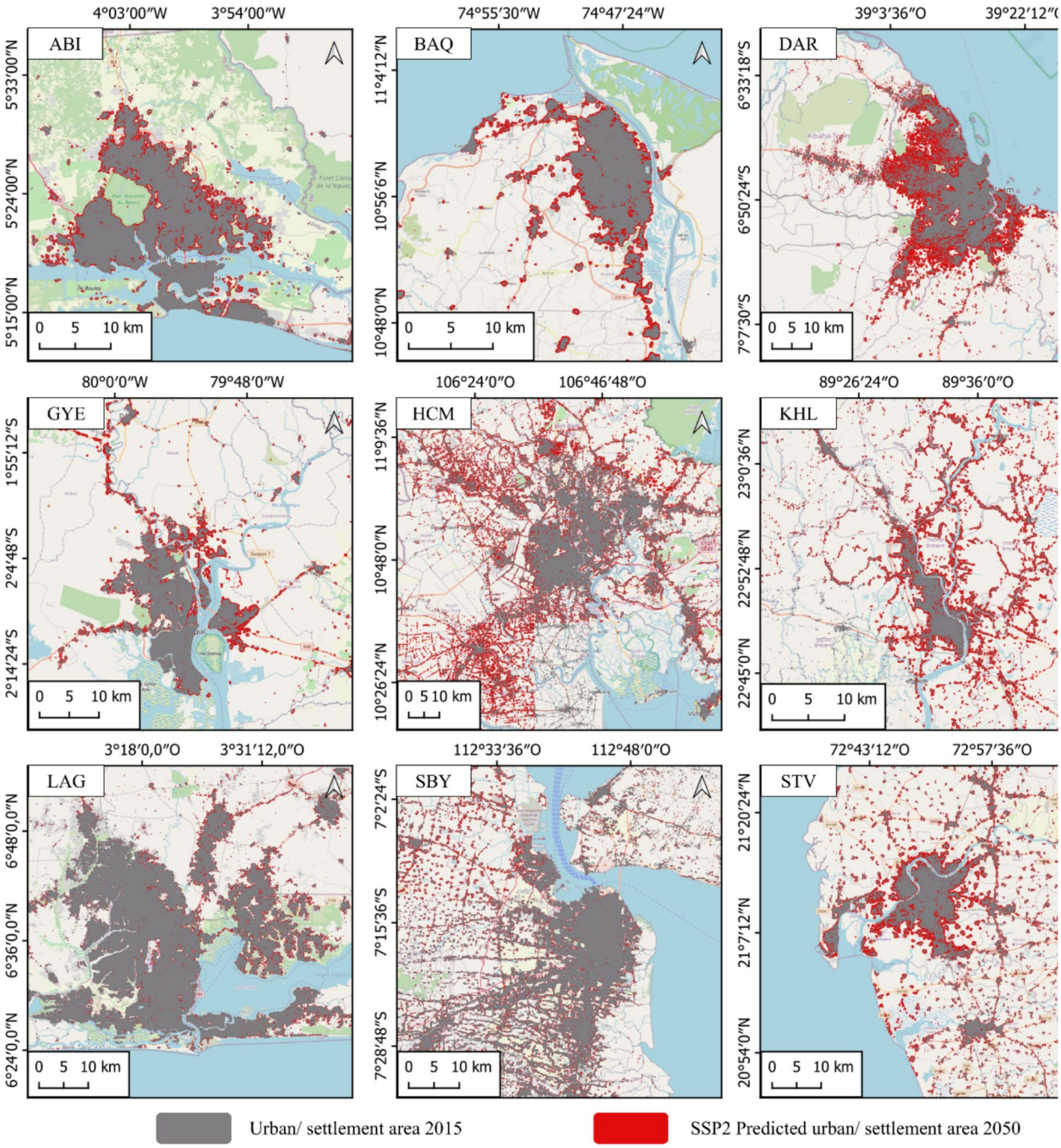

Fig. 8 Projected urban expansion (2016–2050) under the SSP2 scenario. For visualization purposes, only a selected portion of the study area is displayed. Base map: OpenStreetMap & OpenStreetMap-Foundation (CC-BY-SA)

3.3.3 Pluvial flood exposure

Figure 14 depicts the inundation patterns caused by pluvial floods under SSP2/RCP4.5 for 2050, with various shades of blue representing different inundation depths. Among the nine agglomerations, Khulna and Dar es Salaam are expected to experience the highest relative increase, with their flood areas doubling. Pluvial flooding, which affects larger spatial areas than coastal or fluvial floods, disproportionately impacts newly developed urban zones (Fig. 15).

Figure 15 illustrates the projected pluvial flood inundation for a 100-year return period event under SSP1/

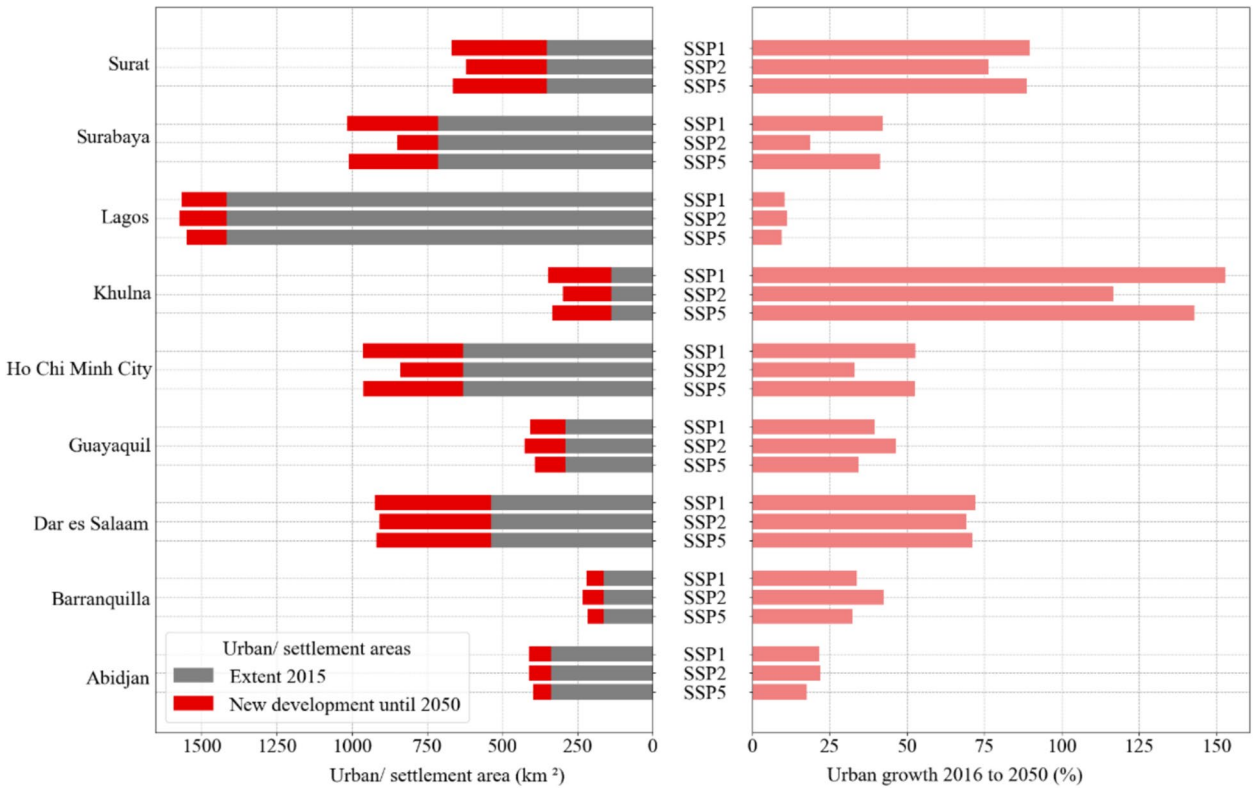

Fig. 9 Quantitative comparison urban growth projections under SSP1, SSP2 and SSP5 scenarios for the study areas of the selected cities. The left panel illustrates urban area and modelled growth, while the right panel presents the percentual growth forecast until 2050

RCP2.6, SSP2/RCP4.5, and SSP5/RCP8.5, offering insights into potential flood-prone areas (Supplementary Table 6). Supplementary Table 7 summarizes the newly developed built-up areas expected to be exposed to flooding by 2050. Among the nine agglomerations, the impact of the SSP/RCP scenarios varies significantly. In most cities, SSP5/RCP8.5 results in the largest pluvial flood extents, except for Guayaquil, Abidjan, and Barranquilla, where SSP2/RCP4.5 yields higher values under the 83rd percentile. For example, Surabaya sees a doubling of flood extent under SSP5/RCP8.5 (40.31/44.00 km^2 for 50th/83rd percentiles) compared to SSP2/RCP4.5 (20.82/22.11 km^2). In contrast, Abidjan and Lagos exhibit minimal scenario-driven differences, with flood extent variations remaining below 0.48 km^2 (50th percentile).

3.3.4 Urban flood contrasts

A comprehensive comparison of flood exposure across nine different cities under three scenarios (SSP1/RCP2.6, SSP2/RCP4.5, and SSP5/RCP8.5, all at the 83rd percentile) and three flood types (coastal, fluvial, and pluvial) highlights key differences in the cities' level of risk to potential flood exposure. Table 4 contrasts flood exposure for the 2015 WSF-based urban extent with the SLEUTH projected urban growth (2016–2050), with values expressed as a percentage of total urban area. Detailed breakdowns of flood exposure can be found in Figs. 11, 13 and 15, as well as in Supplementary Tables 4–7.

In most coastal flooding scenarios, newly developed urban areas are less exposed compared to existing 2015 settlements. However, in Dar es Salaam and Surat, the projected new urban areas will be disproportionately affected, with exposure 2.5–8 times higher than existing areas (Table 4), despite lower overall exposure levels. Surabaya, in particular, is expected to experience a significant increase in flood-prone urban areas, with 83 km^2 affected under SSP5/RCP8.5 (83rd percentile).

For fluvial flooding, exposure affects larger areas than coastal flooding. In Guayaquil, over 37% of newly developed areas (compared to 20% of 2015 urban extents) are projected to be at risk of flood exposure under all scenarios. Ho Chi Minh City and Surabaya also face substantial exposure with 16–30% and 23–30% of their respective 2015 extents and new urban areas affected.

Pluvial flooding shows widespread impacts, with 6–23% of urban areas affected across all scenarios and cities. Disproportionate effects are projected for new

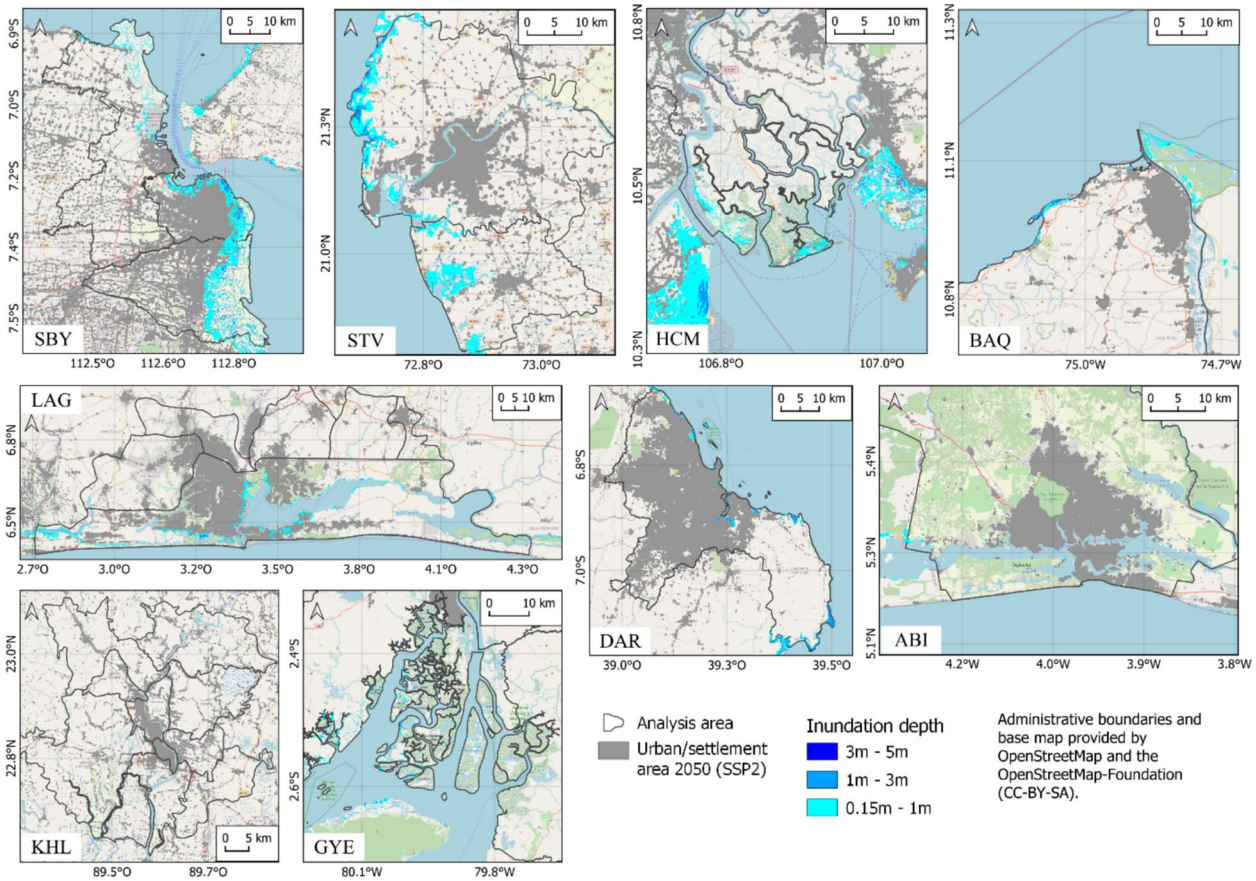

Fig. 10 Projected coastal flooding for 2050 under the SSP2/RCP4.5 scenario (83rd percentile). The flood extent is overlaid with the urban expansion predicted under SSP2, highlighting areas at risk of inundation

urban areas in Abidjan (10.59–13.33%), Dar es Salaam (13.41–13.79%), Guayaquil (20.08–21.16%), and Lagos (13.83–14.35%) (Table 4). Notably, in Dar es Salaam, newly developed urban/settlement areas will face greater flood exposure than existing settlements across all three flood types.

4 Discussion

This study investigates the interplay between urban growth and flood exposure in nine coastal cities across the Global South under different SSP-RCP scenarios. The findings reveal significant variations in urban expansion and risk of flood exposure across the study areas, emphasizing the critical role of socioeconomic and climatic factors in shaping future urban resilience.

4.1 Settlement growth projection

The SLEUTH model was used to predict urban/settlement growth for nine selected agglomerations, incorporating typical input layers historical urban extent data from the WSF. The utilized metrics assess model fit within individual study areas rather than allowing direct comparisons between diverse regions (see Fig. 7). Most cities surpass 0.6 on the Lee-Sallee index, with Khulna recording the lowest value at 0.56, which is still within an acceptable range. Across most cities, AUC values exceeded 0.8, surpassing the 0.75 threshold for favourable simulation accuracy (Verburg et al. 2004; Wu et al. 2008). Khulna, with the lowest AUC (0.73), remains close to this threshold. The reported metrics not only meet but often exceed benchmarks from previous studies (e.g. Saxena and Jat 2020; Kumar and Agrawal 2022). This can be partly attributed to differences in study area characteristics, such as spatial scale and urban morphology. However, the consistently high-quality input from the WSF dataset, which is offering harmonized and reliable urban extent layers, likely played a key role in achieving these results.

To address the challenge of applying consistent, high-resolution urban growth models across large and heterogeneous urban landscapes, we implemented a KDE-based zonation approach combined with spatial tiling (Clarke and Johnson 2020). This methodological adaptation enabled separate calibrations for urban and rural dynamics,

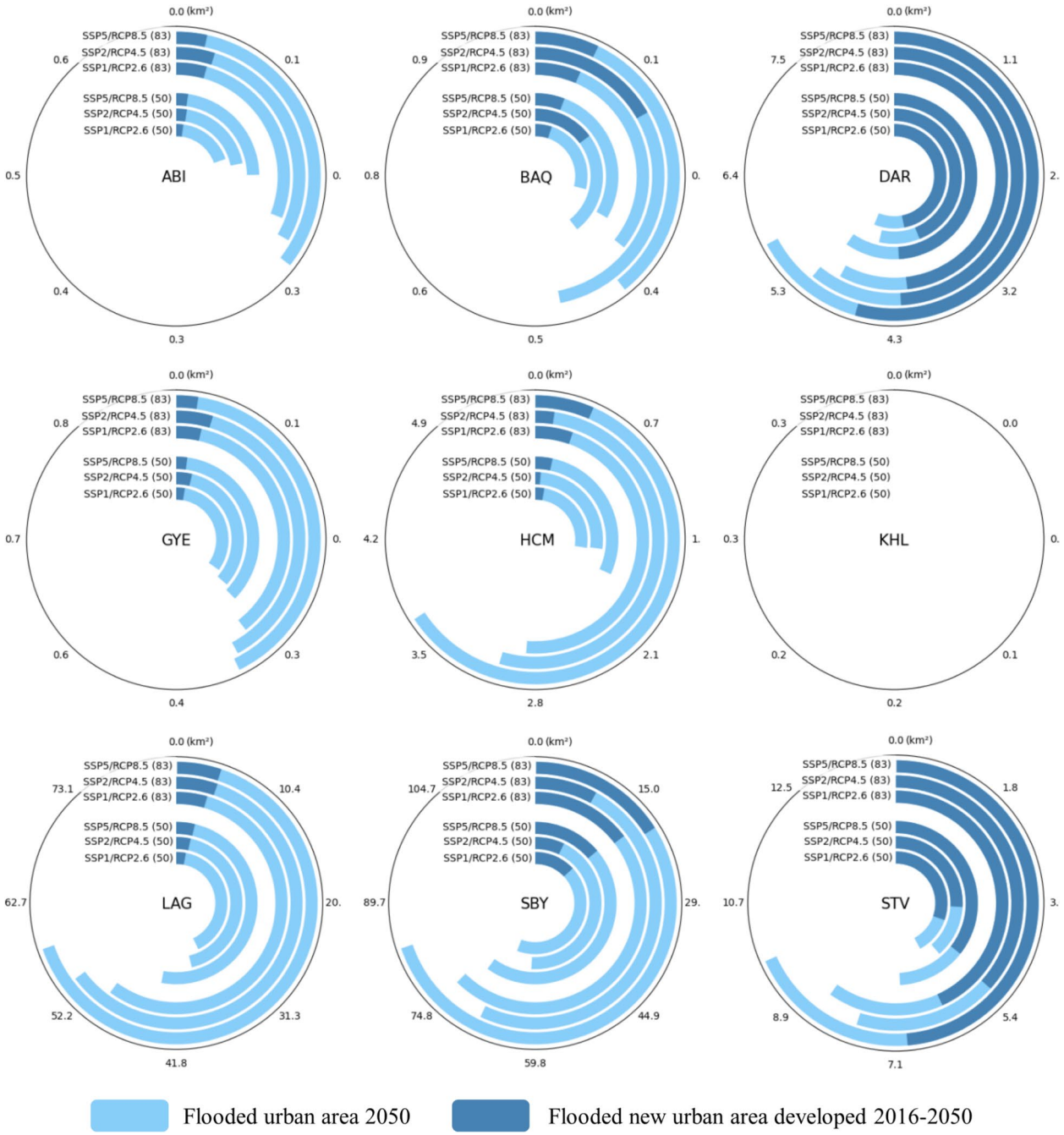

Fig. 11 Projected urban areas exposed to coastal flooding in 2050 across SSP/RCP scenarios. The total urban area at risk of inundation is shown alongside the newly developed urban areas (2016–2050) exposed to flooding. The 50th and 83rd percentiles indicate different flood probability thresholds

improving the SLEUTH model's accuracy (Table 3). By distinguishing between urban cores and rural fringes, the approach captures spatial variability in growth patterns, a critical advancement for scaling urban models to diverse geographic contexts. While our approach distinguishes only between two broad zones—urban cores and rural fringes—this zonation captures a critical spatial dichotomy in growth behavior that improves model calibration. Future work could extend this by incorporating transitional or peri-urban categories to further refine spatial differentiation. For instance, Fig. 8 highlights faster growth rates for compact "urban" cores, while rural

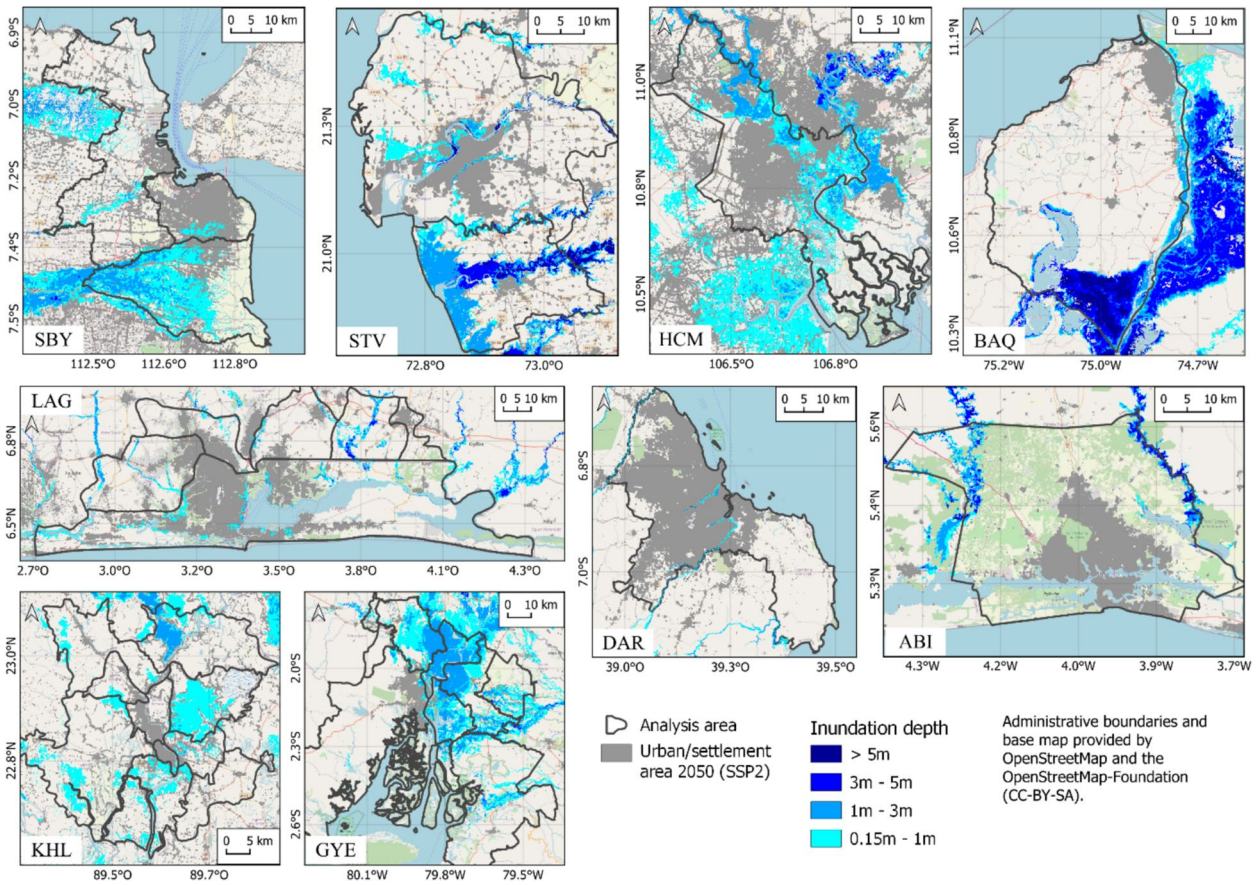

Fig. 12 Projected riverine flooding under the SSP2/RCP4.5 scenario (83rd percentile) overlaid with the 2050 SSP2 urban extent

regions in Ho Chi Minh City and Surabaya exhibit accelerated expansion driven by scattered urban morphology and dense road networks. Overall, these growth trends align with the SSP narratives. For Dar es Salaam, Ho Chi Minh City, Khulna, Surabaya, and Surat SSP2 projects moderate urban population growth, while SSP1 and SSP5 depict more rapid growth in the urban population (Fig. 9). Based on the conducted translation into SLEUTH parameters, this trend in urban population change could be translated into the respective urban growth dynamics. This consistency validates the integration of SSP scenarios into the SLEUTH model (Supplementary Figs. 1 and 2, Jiang and O'Neill 2017). In support of our calibration approach, Clarke and Johnson (2020) demonstrated that spatial autocorrelation exists among SLEUTH calibration coefficients when large datasets are tiled, emphasizing that local spatial dependencies can propagate into urban growth forecasts. This insight further reinforces the need for our zonation approach, as it allows us to account for spatial variability and improve prediction accuracy. However, tiling also introduces methodological challenges. As highlighted by Eyelade et al. (2022), tiling can lead to overfitting within individual tiles at the expense of broader trend recognition across land use categories. In their study of Ibadan, Nigeria, the use of tiled input data improved local fit but reduced the model's ability to capture overarching dynamics. While this finding underscores the need for careful handling of spatial scale and resolution, its generalizability is limited given the study's focus on a single city. Further research is warranted to systematically evaluate the trade-offs of tiling across diverse urban contexts, especially within rapidly urbanizing regions of the Global South.

However, future research is necessary in order to develop quantitative approaches that describe the future shifts from the historical mix of development patterns towards a higher concentration in urban sprawl according to SSP5 or compact development as described in SSP1 in a systematic way.

Four cities – Dar es Salaam, Ho Chi Minh City, Khulna, and Surat – are projected to grow by more than 50% under SSP1 and SSP5 by 2050 compared to 2015 (Fig. 9). Khulna experiences the highest growth, reaching 153.0% in SSP1, 116.6% in SSP2 and 142.9% in SSP5, consistent

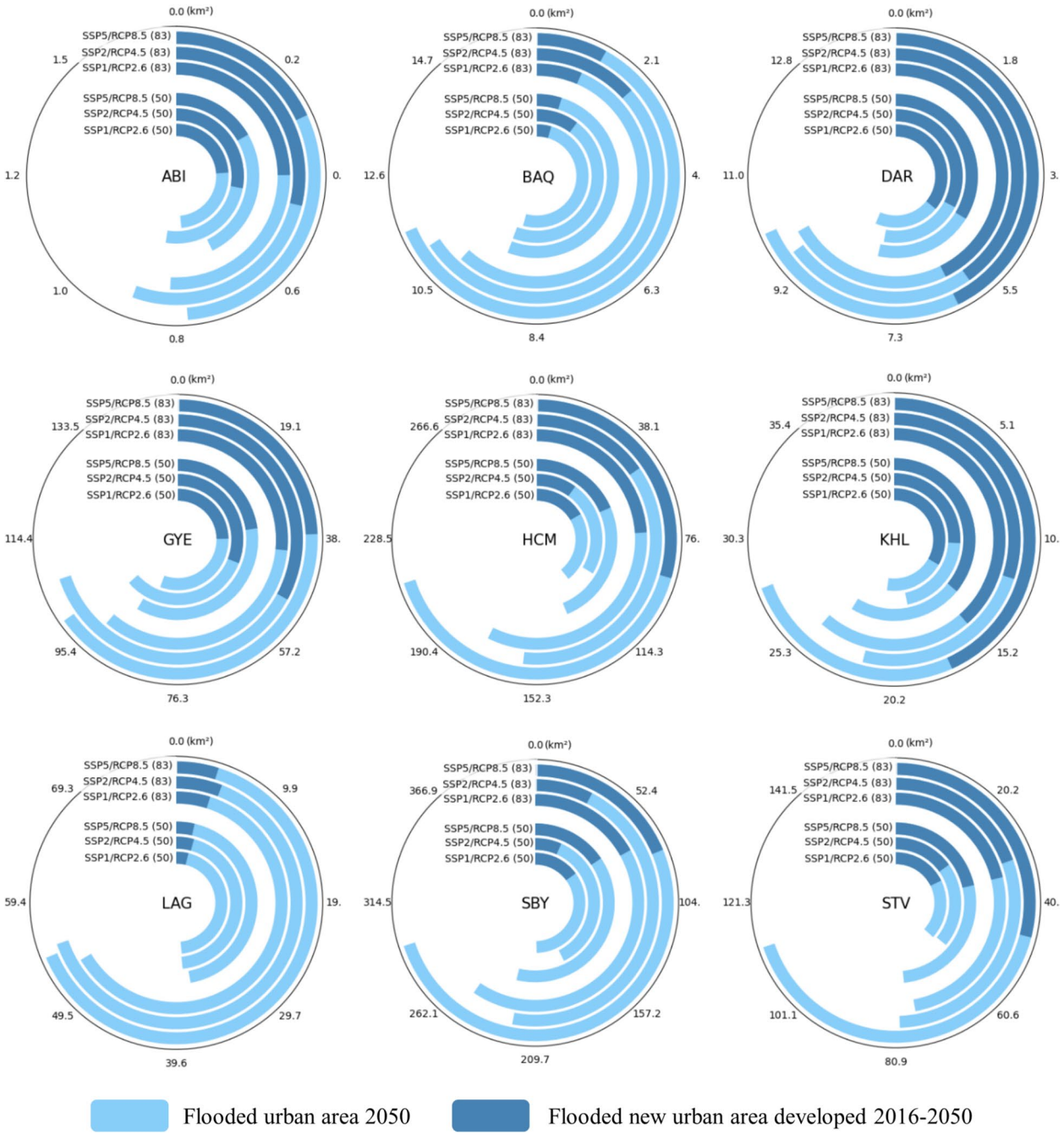

Fig. 13 Total urban area inundated by riverine flooding in 2050 under selected SSP/RCP scenarios, including newly developed flood-exposed urban areas (2016–2050) at the 50th and 83rd percentiles

with its recent rapid expansion. For instance, Alam et al. (2023) report an average annual urban growth of 6.76% in a similar study area between 2010 and 2020. While Alam et al. (2023) analyzed a shorter historical period (2010–2020), their reported annual growth of 6.76% would, if sustained, result in a cumulative increase broadly consistent with our projections. This suggests that our longer-term scenario assumptions remain plausible within the observed urban dynamics. Conversely, Abidjan and Lagos exhibit comparatively lower growth rates. While Lagos' projected growth (10.5% under SSP1, 11.1% under SSP2 and 9.4% under SSP5 between 2016 and 2050) appears low, similar studies confirm this range: Onilude and Vaz (2021) estimated a 0.45% annual growth

Table 4 Proportion of urban/settlement areas potentially exposed to flood across study areas under three scenarios by 2050 (83rd percentile). The table differentiates between pre-existing built-up areas and newly developed areas projected until 2050

City	Scenario	Coastal in %		Fluvial in %		Pluvial in %	
		2015 extent	New area 2016–2050	2015 extent	New area 2016–2050	2015 extent	New area 2016–2050
ABI	SSP1/RCP2.6	0.05	0.04	0.13	0.56	6.25	10.59
	SSP2/RCP4.5	0.06	0.02	0.13	0.64	6.36	10.93
	SSP5/RCP8.5	0.07	0.04	0.15	0.50	6.04	13.33
BAQ	SSP1/RCP2.6	0.19	0.12	5.68	1.98	9.71	12.85
	SSP2/RCP4.5	0.19	0.25	5.40	3.21	10.26	14.25
	SSP5/RCP8.5	0.20	0.14	6.22	2.54	11.18	14.13
DAR	SSP1/RCP2.6	0.15	1.06	0.66	1.62	7.13	13.41
	SSP2/RCP4.5	0.19	1.13	0.67	1.59	7.28	13.57
	SSP5/RCP8.5	0.20	1.21	0.70	1.64	7.45	13.79
GYE	SSP1/RCP2.6	0.11	0.03	18.14	35.13	16.61	20.08
	SSP2/RCP4.5	0.11	0.03	19.30	37.21	17.58	21.44
	SSP5/RCP8.5	0.12	0.02	21.33	37.17	18.01	21.16
HCM	SSP1/RCP2.6	0.41	0.09	16.09	21.94	13.25	12.96
	SSP2/RCP4.5	0.47	0.06	17.58	22.39	14.26	13.56
	SSP5/RCP8.5	0.53	0.11	19.51	27.08	15.03	14.57
KHL	SSP1/RCP2.6	0.00	0.00	6.67	7.40	7.10	7.49
	SSP2/RCP4.5	0.00	0.00	7.03	7.57	7.73	7.49
	SSP5/RCP8.5	0.00	0.00	7.67	8.89	8.11	8.29
LAG	SSP1/RCP2.6	3.28	2.52	3.44	2.62	10.12	13.83
	SSP2/RCP4.5	3.51	2.81	3.57	2.96	10.32	14.25
	SSP5/RCP8.5	3.81	3.23	3.57	2.86	10.53	14.35
SBY	SSP1/RCP2.6	7.99	5.83	24.99	23.56	14.39	13.48
	SSP2/RCP4.5	8.23	7.17	26.62	23.87	15.31	16.54
	SSP5/RCP8.5	9.00	6.51	30.06	26.61	16.21	14.92
STV	SSP1/RCP2.6	0.68	1.96	11.88	10.89	21.54	17.99
	SSP2/RCP4.5	0.74	1.95	13.82	11.67	22.32	18.36
	SSP5/RCP8.5	0.80	2.23	18.76	15.01	22.99	19.21
Exposure of newly developed area (%) is more than 10% less than the exposure of the 2015 extent (%)		Exposure of newly developed areas (%) within the same range of exposure (± 10%) than the 2015 extent (%)		Exposure of newly developed areas (%) is between 10% to + 100% higher than the exposure of the 2015 extent (%)		Exposure of newly developed areas (%) is more than 100% higher than the exposure of the 2015 extent (%)	

rate (2010–2030) using a CA Markov Chain model, while Gilbert and Shi (2023) projected 0.74% annual growth (2020–2040). For Abidjan, Wang et al. (2022) modelled an annual growth rate of 1.2% for the period 2016–2025, although based on a shorter timeframe and somewhat lower rates, this steady urban expansion trend aligns qualitatively with our cumulative growth projections of 21.6%, 22.0% and 17.5% by 2050 under SSP1, SSP2, and SSP5, respectively. The differences may reflect variation in temporal scope, spatial resolution, and modelling assumptions.

On a national scale, Wolff et al. (2023) analysed SSP-based projections of urban extent until 2100 and found that the highest urban expansion varies across European countries. In most cases, SSP5 results in the largest urban extent, while SSP1 and SSP2 occupy intermediate positions. However, the European narratives cannot be directly compared to our findings, as our study focuses on cities in the Global South, where urbanization dynamics, socio-economic drivers, and climate vulnerabilities differ significantly. This underscores the need for region-specific analyses.

4.2 Flood exposure scenario assessment

To asses urban flood exposure, projected 2050 urban extents are overlaid onto the flood scenarios for SSP1/

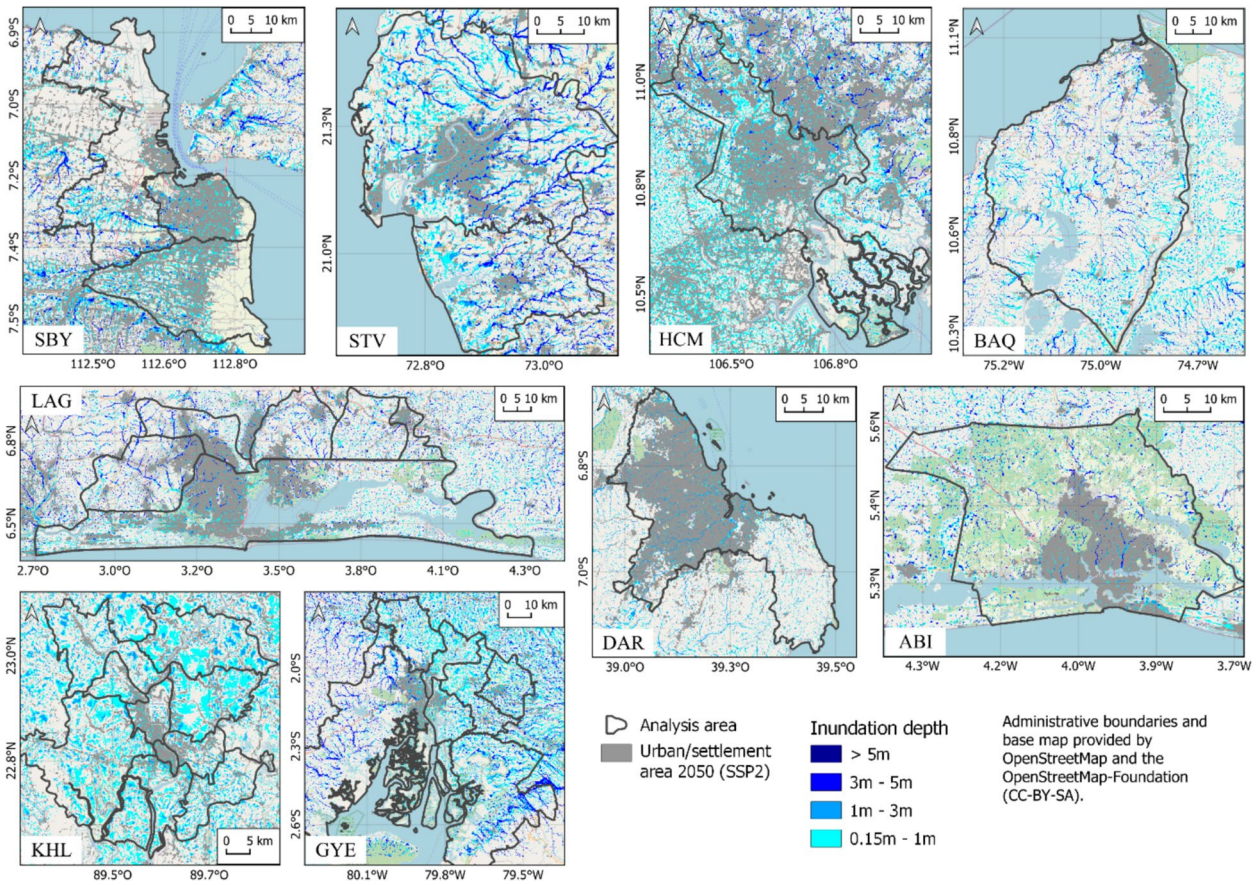

Fig. 14 Projected pluvial flooding for the SSP2/RCP4.5 scenario (83rd percentile) overlaid with the 2050 SSP2 urban extent

RCP2.6, SSP2/RCP4.5, and SSP5/RCP8.5, considering both the 50th and 83rd percentiles for a 100-year return period. The interplay between urban population growth and climate change creates complex scenario-driven patterns, leading to varying flood extents across different cities and flood types.

The impact of SSP/RCP scenarios varies significantly across the nine study areas, reflecting divergent urbanization dynamics and climatic sensitivities. For example, Barranquilla and Guayaquil exhibit the lowest flood exposure under SSP1/RCP2.6 across all flood types, while Khulna and Surabaya experience reduced flood hazard exposure under SSP2/RCP4.5 due to slower urban population growth and moderate climate forcing. Conversely, Guayaquil faces the highest fluvial and pluvial flooding SSP2/RCP4.5, highlighting the non-linear relationship between urban expansion and flood hazard extent. Notably, SSP5/RCP8.5 results in the lowest fluvial and pluvial flood exposure for Abidjan but the highest for SSP1/RCP2.6, a divergence attributed to lower total population projections under SSP5 (Supplementary Table 2). These findings align with Sun et al. (2022), who emphasize the critical role of urban growth scenarios in shaping future flood exposure.

4.3 Implications of SSP/RCP-based flood exposure assessment

The 2050 flood assessment reveals distinct patterns of urban flood exposure in the Global South, where rapid urbanization amplifies exposure to coastal, fluvial and pluvial flooding. Under all flood types, in several cities, newly developed urban areas exhibit markedly higher flood exposure—up to 8 times greater than in existing areas (e.g., Dar es Salaam, Surat)—underscoring the risks of non-risk-informed expansion (Mahtta et al. 2022). However, this trend is not consistent across all study sites, with some cities showing comparable or lower exposure in new developments, pointing to the influence of localized topographic and planning factors. For instance, Dar es Salaam and Surat exhibit 2.5–8 times higher exposure in new developments compared to existing urban areas, highlighting the urgency of risk-informed land-use planning. Surabaya's coastal flooding (up to 83 km^2 under SSP5/RCP8.5) and Guayaquil's

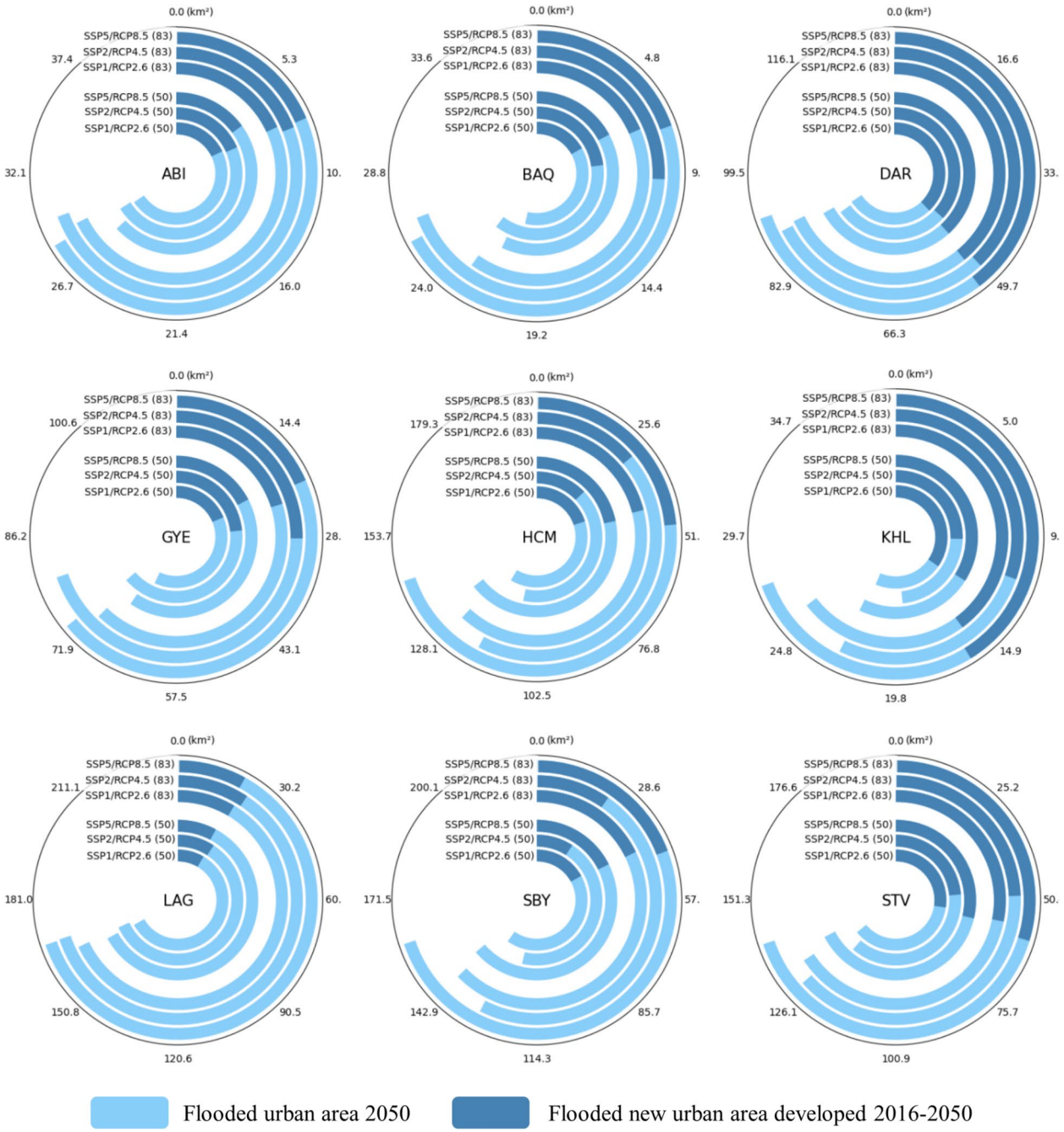

Fig. 15 Total urban area affected by pluvial flooding in 2050 under the selected SSP/RCP scenarios, including newly developed flood-exposed areas (2016–2050) at the 50th and 83rd percentiles

fluvial exposure (37% of new urban areas) demand targeted interventions. This highlights the urgent need for strategic urban planning that avoids flood-prone areas and strengthens long-term urban resilience. Context-specific resilience strategies are essential to address the varied exposure patterns observed across different cities and flood types. Pluvial flooding, which affects larger spatial areas (e.g., 10.53–21.16% of new urban areas in Abidjan and Guayaquil), underscores the importance of considering rain-induced flooding in future urban planning. The persistence of high exposure in newly developed zones highlights the limitations of relying solely on climate mitigation and emphasizes the role of proactive urban design.

In some cases, newly developed areas may appear less exposed, which can be explained by several factors: generally low overall exposure levels, historical settlement patterns that avoided high-risk zones but may face increasing risk of flood exposure under future climate conditions, and future urban expansion into inland areas with lower flood exposure but potentially unfavourable topography. These variations highlight the case-specific nature of future exposure and underscore the importance of spatially explicit, scenario-based assessments.

Ultimately, while high radiative forcing scenarios exacerbate flood exposure, socioeconomic pathways shaping urban expansion are equally critical. These findings align with Hemmati et al. (2020), who stress the importance of urban growth management in building flood resilience. By linking scenario-based assessments to localized strategies, this study provides actionable insights for policymakers navigating the dual challenges of urbanization and climate change.

These findings underscore broader trends across the Global South: the compounding vulnerabilities of informal expansion, limited infrastructure investment, and weak enforcement of spatial planning. The integration of scenario-based models into local planning frameworks offers a promising pathway to anticipate risks and design proactive, climate-resilient urban strategies (Horn 2020).

4.4 Understanding methodological boundaries

This study relies on various assumptions and is subject to modelling uncertainties. The SSPs, originally designed at the national scale, lack adaptation to local study areas. Their integration into the SLEUTH model via Breed and Spread coefficients is an uncommon approach (Jones and O'Neill, 2016), introducing potential uncertainties. While the IIASA urbanization projections primarily focus on demographic trends rather than spatial land expansion, their integration into the SLEUTH model provides a proxy for future urban growth by adjusting the Breed and Spread coefficients. However, this approach assumes a correlation between population development and urban extent, which may not fully capture variations in urban density, land-use policies, and infrastructure constraints. Future studies could enhance this framework by incorporating additional land-use change datasets to refine the spatial accuracy of urban expansion projections.

Further uncertainties arise from SLEUTH input data, climate scenarios, the DEM, and the flood defence parameters in the Fathom flood dataset. For instance, another widely used tool, the Aqueduct Global Flood Analyzer projects near-complete inundation of Khulna by 2050 under a BaU scenario for a 100-year coastal flood event (WRI Aqueduct 2023). In contrast, this study did not simulate any coastal flooding for Khulna. This discrepancy highlights how strongly model outcomes depend on the selected input data, assumptions, and methods, underlining the importance of understanding model limitations when interpreting flood hazard projections.

This study also relies on the defended-status flooding datasets, which assume the presence of flood protection infrastructure. While this approach aims to provide the most realistic flood exposure assessment given the available data, the completeness of flood-defence infrastructure information for the selected cities cannot be independently verified. This limitation may affect intercity comparisons, as some regions might have better-documented flood defences than others. Additionally, this study assesses coastal, fluvial, or pluvial floods separately, excluding compound flood events, which simplifies, but does not fully capture, the complexity of real extreme events. However, our study aligns with current best practices (see Introduction), employing zonation in SLEUTH modelling to improve predictive accuracy and integrating SSP/RCP perspectives beyond most existing studies. Despite these limitations, the study's methodological setup effectively addresses the research questions and provides insights into future urban flood exposure.

Another critical consideration is the levee effect, which refers to the tendency of populations to concentrate in areas perceived as protected due to flood defence infrastructure (Haer et al. 2020; Mård et al. 2018). While this effect is not incorporated in the flood exposure scenarios, its influence on future urban expansion patterns remains an important factor. If flood defences fail or prove insufficient under extreme conditions, these areas could experience disproportionate flood impacts due to high population densities. Understanding how this dynamic shapes settlement patterns will be essential for refining future flood risk assessments. Future work should incorporate behavioral modeling to assess how perceived safety from levees might attract denser settlement in flood-prone areas, potentially amplifying future exposure. This dynamic is especially critical in rapidly urbanizing contexts with limited risk communication and enforcement.

5 Conclusions

This study presents a comprehensive urban growth prediction and future flood exposure assessment for nine coastal cities across three continents, addressing the complex interplay of urbanization, climate change, and flood risk in the Global South. By integrating SSPs into a refined SLEUTH model enhanced with KDE-based zonation, we offer a context-specific, spatially explicit approach to predicting urban expansion and flood exposure at a high resolution (30 m). The inclusion of

a diverse set of study areas, spanning varied climatic, socioeconomic, and geographic contexts, enables a cross-continental comparative analysis, revealing critical insights into how urbanization and climate change jointly shape potential flood exposure.

Notably, in some cities such as Dar es Salaam and Surat, newly developed urban areas face disproportionately higher flood exposure than existing settlements – by a factor of 2.5–8 – underscoring the risks of non-risk-informed planning in those contexts. These findings highlight that future flood exposure are driven not only by high radiative forcing scenarios but also by socioeconomic pathways shaping urban expansion. This dual dependency emphasizes the need for integrated strategies combining climate change mitigation with proactive, scenario-based urban planning.

Central to these findings is the imperative for cities to be assessed individually, balancing their unique physical and socioeconomic contexts with projected development trajectories. For decision-makers, this underscores the value of localized data and adaptive governance. While global datasets provide broad insights, tailored strategies, which are accounting for governance structures, topography, and community vulnerabilities, are critical for resilience.

Ultimately, as cities navigate the challenges of the Anthropocene, integrating urban modelling with climate projections can provide a roadmap for more sustainable and adaptive urban growth. By identifying high-risk areas and potential mitigation pathways, this study advances a more informed and proactive approach to urban resilience, ensuring that coastal cities in the Global South can adapt to both rising seas and rapid urbanization.

Supplementary Information

The online version contains supplementary material available at https://doi.org/10.1007/s44218-025-00109-6.

Supplementary Material 1.

Acknowledgements
We thank OpenStreetMap and the OpenStreetMap-Foundation for providing a basemap service under the CC-BY-SA license. Further details are available at: https://www.openstreetmap.org/copyright/en. We extend our gratitude to Fathom (formerly SSBN) for supplying Global Flood Map data under the requested scenarios for our study sites. We thank two anonymous reviewers for their critical and helpful remarks on a previous version of this manuscript.

Authors' contributions
Conceptualization: Felix Bachofer, Claudia Kuenzer; Methodology: Felix Bachofer, Zhiyuan Wang; Formal analysis and investigation: Felix Bachofer, Andrea Reimuth, Zhiyuan Wang; Writing—original draft preparation: Felix Bachofer, Andrea Reimuth, Zhiyuan Wang; Writing—review and editing: Juliane Huth, Christina Eisfelder, Andrea Reimuth, Claudia Kuenzer. All authors have read and approved the final version of the manuscript.

Funding
This work was supported by internal funding from the German Aerospace Center (DLR). The authors did not receive support from any third-party organization for the submitted work.

Data availability
The World Settlement Footprint (WSF) data is accessible via DLR's EOC Geoservice (https://geoservice.dlr.de). The urban/settlement growth modelling results have been deposited in the ZENODO open data repository under a CC-BY license (https://doi.org/10.5281/zenodo.10605458).

Declarations

Competing interests
The authors declare no competing interests relevant to the content of this article.

Author details
[1]German Aerospace Center (DLR), Earth Observation Center (EOC), Muenchener Strasse 20, 82234 Wessling, Germany. [2]Ludwig-Maximilians Universität München, Department of Geography, Luisenstrasse 37, 80333 Munich, Germany. [3]University of Würzburg, Institute of Geography and Geology, Department of Remote Sensing, Am Hubland, 97074 Würzburg, Germany.

Received: 31 January 2024 Revised: 14 August 2025 Accepted: 21 October 2025
Published online: 12 January 2026

References

Airbus (2019) Copernicus DEM Copernicus Digital Elevation Model - Product Handbook. Contract No.: AO/1–9422/18/I-LG

Alam I, Nahar K, Morshed MM (2023) Measuring urban expansion pattern using spatial matrices in Khulna City, Bangladesh. Heliyon 9(2):e13193. https://doi.org/10.1016/j.heliyon.2023.e13193

Alfieri L, Burek P, Dutra E, Krzeminski B, Muraro D, Thielen J, Pappenberger F (2013) GloFAS – global ensemble streamflow forecasting and flood early warning. Hydrol Earth Syst Sci 17(3):1161–1175. https://doi.org/10.5194/hess-17-1161-2013

Barragán JM, de Andrés M (2015) Analysis and trends of the world's coastal cities and agglomerations. Ocean Coast Manage 114:11–20. https://doi.org/10.1016/j.ocecoaman.2015.06.004

Bates P (2022) Uneven burden of urban flooding. Nat Sustain 6(1):9–10. https://doi.org/10.1038/s41893-022-01000-9

Bernard A, Long N, Becker M, Khan J, Fanchette S (2022) Bangladesh's vulnerability to cyclonic coastal flooding. Nat Hazards Earth Syst Sci 22(3):729–751. https://doi.org/10.5194/nhess-22-729-2022

Center for International Earth Science Information Network CIESIN, Columbia University, Information Technology Outreach Services ITOS, University of Georgia (2013) Global Roads Open Access Data Set, Version 1 (gROADSv1). In: (SEDAC) NSDaAC, editor. Palisades, NY, USA

Chaudhuri G, Clarke KC (2013) The SLEUTH land use change model: a review. Int J Environ Resources Res 1(1):88–105. https://doi.org/10.22069/ijerr.2013.1688

Chen G, Li X, Liu X, Chen Y, Liang X, Leng J, Xu X, Liao W, Qiu Y, Wu Q, Huang K (2020) Global projections of future urban land expansion under shared socioeconomic pathways. Nat Commun 11(1):537. https://doi.org/10.1038/s41467-020-14386-x

Chen S, Huang Q, Muttarak R, Fang J, Liu T, He C, Liu Z, Zhu L (2022) Updating global urbanization projections under the shared socioeconomic pathways. Sci Data 9(1):137. https://doi.org/10.1038/s41597-022-01209-5

Clarke KC (2018) Land Use Change Modeling with SLEUTH: Improving Calibration with a Genetic Algorithm. In: Camacho Olmedo MT, Paegelow M, Mas J-F, Escobar F (eds) Geomatic Approaches for Modeling Land Change Scenarios. Springer International Publishing, Cham, pp 139–161

Clarke KC, Hoppen S, Gaydos L (1997) A self-modifying cellular automaton model of historical urbanization in the San Francisco Bay Area. Environ Plann B Plann des 24(2):247–261. https://doi.org/10.1068/b240247
Clarke KC, Johnson JM (2020) Calibrating SLEUTH with big data: projecting California's land use to 2100. Computers, Environment and Urban Systems 83. https://doi.org/10.1016/j.compenvurbsys.2020.101525
Clarke KC, Hoppen S, Gaydos LJ (1996) Methods and techniques for rigorous calibration of a cellular automaton model of urban growth. Third International Conference/Workshop on Integrating GIS and Environmental Modeling: 1319–1328.
Clarke KC, Dietzel C, Goldstein NC, editors. (2004) A Decade of SLEUTHing: Lessons Learned from Applications of a Cellular Automaton Land Use Change Model
Copernicus Sentinel data (2020). Copernicus Sentinel 1 and 2. In: Agency pbES, editor.
Corbane C, Pesaresi M, Kemper T, Politis P, Florczyk AJ, Syrris V, Melchiorri M, Sabo F, Soille P (2019) Automated global delineation of human settlements from 40 years of Landsat satellite data archives. Big Earth Data 3(2):140–169. https://doi.org/10.1080/20964471.2019.1625528
Couasnon A, Scussolini P, Tran TVT, Eilander D, Muis S, Wang H, Keesom J, Dullaart J, Xuan Y, Nguyen HQ, Winsemius HC, Ward PJ (2022) A Flood Risk Framework Capturing the Seasonality of and Dependence Between Rainfall and Sea Levels—An Application to Ho Chi Minh City. Vietnam. Water Resources Research 58(2):e2021WR030002. https://doi.org/10.1029/2021wr030002
Crespo Cuaresma J (2017) Income projections for climate change research: a framework based on human capital dynamics. Glob Environ Change 42:226–236. https://doi.org/10.1016/j.gloenvcha.2015.02.012
Dasgupta S, Laplante B, Murray S, Wheeler D (2010) Exposure of developing countries to sea-level rise and storm surges. Clim Change 106(4):567–579. https://doi.org/10.1007/s10584-010-9959-6
Dellink R, Chateau J, Lanzi E, Magné B (2017) Long-term economic growth projections in the Shared Socioeconomic Pathways. Glob Environ Change 42:200–214. https://doi.org/10.1016/j.gloenvcha.2015.06.004
Dietzel C, Clarke KC (2007) Toward Optimal Calibration of the SLEUTH Land Use Change Model. Transact GIS 11(1):29–45. https://doi.org/10.1111/j.1467-9671.2007.01031.x
Dodman D, Hayward B, Pelling M, Broto VC, Chow W, Chu E, Dawson R, Khirfan L, McPhearson T, Prakash A, Zheng Y, Ziervogel G (2023) Cities, Settlements and Key Infrastructure. In: Pörtner H-O, Roberts DC, Tignor M, Poloczanska ES, Mintenbeck K, Alegría A et al (eds) Contribution of Working Group II to the Sixth Assessment Report of the Intergovernmental Panel on Climate Change: Climate Change 2022 – Impacts, Adaptation and Vulnerability. Cambridge University Press, Cambridge, UK and New York, NY, USA, pp 907–1040
Edmonds DA, Caldwell RL, Brondizio ES, Siani SMO (2020) Coastal flooding will disproportionately impact people on river deltas. Nat Commun 11(1):4741. https://doi.org/10.1038/s41467-020-18531-4
European Space Agency and Airbus (2022) Copernicus DEM. In: Agency ES, editor.
Eyelade D, Clarke KC, Ijagbone I (2022) Impacts of spatiotemporal resolution and tiling on SLEUTH model calibration and forecasting for urban areas with unregulated growth patterns. Int J Geogr Inf Sci 36(5):1037–1058. https://doi.org/10.1080/13658816.2021.2011292
Eyring V, Bony S, Meehl GA, Senior CA, Stevens B, Stouffer RJ, Taylor KE (2016) Overview of the coupled model intercomparison project phase 6 (CMIP6) experimental design and organization. Geosci Model Dev 9(5):1937–1958. https://doi.org/10.5194/gmd-9-1937-2016
Fathom (2022a) Fathom - Global 3.0 Methods: In brief
Fathom (2022b) Fathom launches new Global Flood Map – Fathom-Global 3.0 Bristol, UKAvailable from: https://www.fathom.global/newsroom/fathom-launches-global-flood-map/. Accessed 23.08.2023
Fathom (2023) Fathom Global Flood Map Specification Bristol, UKAvailable from: https://www.fathom.global/product/global-flood-map/. Accessed 30.06.2023
Feng H-H, Liu H-P, Lü Y (2012) Scenario prediction and analysis of urban growth using SLEUTH model. Pedosphere 22(2):206–216. https://doi.org/10.1016/s1002-0160(12)60007-1
Florczyk AJ, Corbane C, Ehrlich D, Freire S, Kemper T, Maffenini L, Melchiorri M, Pesaresi M, Politis P, Schiavina M, Sabo F, Zanchetta L (2019) GHSL Data Package 2019. European Commission, Joint Research Centre (JRC). Contract No.: JRC 117104
Fricko O, Havlik P, Rogelj J, Klimont Z, Gusti M, Johnson N, Kolp P, Strubegger M, Valin H, Amann M, Ermolieva T, Forsell N, Herrero M, Heyes C, Kindermann G, Krey V, McCollum DL, Obersteiner M, Pachauri S, Rao S, Schmid E, Schoepp W, Riahi K (2017) The marker quantification of the shared socioeconomic pathway 2: a middle-of-the-road scenario for the 21st century. Glob Environ Change 42:251–267. https://doi.org/10.1016/j.gloenvcha.2016.06.004
Gao J, O'Neill B (2019) Data-driven spatial modeling of long-term urban land development potential for global environmental change impact assessment: the SELECT model. Environ Model Softw. https://doi.org/10.1016/j.envsoft.2019.06.015
Gao J, O'Neill BC (2020) Mapping global urban land for the 21st century with data-driven simulations and shared socioeconomic pathways. Nat Commun 11(1):2302. https://doi.org/10.1038/s41467-020-15788-7
Gilbert KM, Shi Y (2023) Urban growth monitoring and prediction using remote sensing urban monitoring indices approach and integrating CA-Markov model: a case study of Lagos City, Nigeria. Sustainability 16(1):30. https://doi.org/10.3390/su16010030
Glavovic BC, Dawson R, Chow W, Garschagen M, Haasnoot M, Singh C, Thomas A (2022) Cross-Chapter Paper 2: Cities and Settlements by the Sea. In: Pörtner H-O, Roberts DC, Tignor M, Poloczanska ES, Mintenbeck K, Alegría A et al (eds) Contribution of Working Group II to the Sixth Assessment Report of the Intergovernmental Panel on Climate Change: Climate Change 2022 – Impacts, Adaptation and Vulnerability. Cambridge University Press, Cambridge, UK and New York, NY, USA, pp 2163–2194
Goncalves TM, Zhong X, Ziggah YY, Dwamena BY (2019) Simulating urban growth using cellular automata approach (SLEUTH)-a case study of Praia City, Cabo Verde. IEEE Access 7:156430–156442. https://doi.org/10.1109/access.2019.2949689
Gong P, Liu H, Zhang M, Li C, Wang J, Huang H, Clinton N, Ji L, Li W, Bai Y, Chen B, Xu B, Zhu Z, Yuan C, Ping Suen H, Guo J, Xu N, Li W, Zhao Y, Yang J, Yu C, Wang X, Fu H, Yu L, Dronova I, Hui F, Cheng X, Shi X, Xiao F, Liu Q, Song L (2019) Stable classification with limited sample: transferring a 30-m resolution sample set collected in 2015 to mapping 10-m resolution global land cover in 2017. Sci Bull 64(6):370–373. https://doi.org/10.1016/j.scib.2019.03.002
Gong P, Li X, Wang J, Bai Y, Chen B, Hu T, Liu X, Xu B, Yang J, Zhang W, Zhou Y (2020) Annual maps of global artificial impervious area (GAIA) between 1985 and 2018. Remote Sen Environ 236:111510. https://doi.org/10.1016/j.rse.2019.111510
Haer T, Husby TG, Botzen WJW, Aerts JCJH (2020) The safe development paradox: an agent-based model for flood risk under climate change in the European Union. Global Environ Change 60:102009. https://doi.org/10.1016/j.gloenvcha.2019.102009
Hallegatte S, Green C, Nicholls RJ, Corfee-Morlot J (2013) Future flood losses in major coastal cities. Nat Clim Change 3(9):802–806. https://doi.org/10.1038/nclimate1979
Hanley JA, McNeil BJ (1982) The meaning and use of the area under a receiver operating characteristic (ROC) curve. Radiology 143(1):29–36. https://doi.org/10.1148/radiology.143.1.7063747
Hanson S, Nicholls R, Ranger N, Hallegatte S, Corfee-Morlot J, Herweijer C, Chateau J (2010) A global ranking of port cities with high exposure to climate extremes. Clim Change 104(1):89–111. https://doi.org/10.1007/s10584-010-9977-4
Haque A, Nicholls RJ (2018) Floods and the Ganges-Brahmaputra-Meghna Delta. In: Nicholls RJ, Hutton CW, Adger WN, Hanson SE, Rahman MM, Salehin M (eds) Ecosystem Services for Well-Being in Deltas: Integrated Assessment for Policy Analysis. Springer International Publishing, Cham, pp 147–159
Harb M, Garschagen M, Cotti D, Krätzschmar E, Baccouche H, Ben Khaled K, Bellert F, Chebil B, Ben Fredj A, Ayed S, Shekhar H, Hagenlocher M (2020) Integrating data-driven and participatory modeling to simulate future urban growth scenarios: findings from Monastir, Tunisia. Urban Sci 4(1):10. https://doi.org/10.3390/urbansci4010010
Hawker L, Uhe P, Paulo L, Sosa J, Savage J, Sampson C, Neal J (2022) A 30 m global map of elevation with forests and buildings removed. Environ Res Lett 17(2):024016. https://doi.org/10.1088/1748-9326/ac4d4f

He W, Li X, Zhou Y, Shi Z, Yu G, Hu T, Wang Y, Huang J, Bai T, Sun Z, Liu X, Gong P (2023) Global urban fractional changes at a 1 km resolution throughout 2100 under eight scenarios of shared socioeconomic pathways (SSPs) and representative concentration pathways (RCPs). Earth Syst Sci Data 15(8):3623–3639. https://doi.org/10.5194/essd-15-3623-2023

Hemmati M, Ellingwood BR, Mahmoud HN (2020) The role of urban growth in resilience of communities under flood risk. Earths Future 8(3):e2019EF001382. https://doi.org/10.1029/2019EF001382

Horn A (2020) Reviewing implications of urban growth management and spatial governance in the Global South. Plann Pract Res 35(4):452–465. https://doi.org/10.1080/02697459.2020.1757228

Huang X, Song Y, Yang J, Wang W, Ren H, Dong M, Feng Y, Yin H, Li J (2022) Toward accurate mapping of 30-m time-series global impervious surface area (GISA). Int J Appl Earth Observ Geoinform 109:102787. https://doi.org/10.1016/j.jag.2022.102787

IFRC (2023) DREF Operation - Final Report Ecuador Floods. International Federation of Red Cross and Red Crescent Societies (IFRC) 03(05):2023

IIASA (2018) SSP Database (Shared Socioeconomic Pathways) - Version 2.0. In: (IIASA) IIfASA, editor

IPCC (2023) Climate change 2022 – impacts, adaptation and vulnerability: working group II contribution to the sixth assessment report of the Intergovernmental Panel on Climate Change. Cambridge University Press, Cambridge

Jamshed A, Patel C, Puriya A, Iqbal N, Rana IA, McMillan JM, Pandey R, Altaf S, Mehmood RT, Ub S (2023) Flood resilience assessment from the perspective of urban (in)formality in Surat. Implications for sustainable development. Nat Hazards, India. https://doi.org/10.1007/s11069-023-06267-5

Jantz CA, Goetz SJ, Shelley MK (2016) Using the sleuth urban growth model to simulate the impacts of future policy scenarios on urban land use in the Baltimore-Washington Metropolitan Area. Environ Plann B Plann des 31(2):251–271. https://doi.org/10.1068/b2983

Jiang L, O'Neill BC (2017) Global urbanization projections for the shared socioeconomic pathways. Glob Environ Change 42:193–199. https://doi.org/10.1016/j.gloenvcha.2015.03.008

Jibhakate SM, Timbadiya PV, Patel PL (2023) Multiparameter flood hazard, socioeconomic vulnerability and flood risk assessment for densely populated coastal city. J Environ Manage 344:118405. https://doi.org/10.1016/j.jenvman.2023.118405

Jones B, O'Neill BC (2016) Spatially explicit global population scenarios consistent with the Shared Socioeconomic Pathways. Environ Res Lett 11(8):084003. https://doi.org/10.1088/1748-9326/11/8/084003

Kc S, Lutz W (2017) The human core of the shared socioeconomic pathways: population scenarios by age, sex and level of education for all countries to 2100. Glob Environ Change 42:181–192. https://doi.org/10.1016/j.gloenvcha.2014.06.004

Kebede AS, Nicholls RJ (2011) Exposure and vulnerability to climate extremes: population and asset exposure to coastal flooding in Dar es Salaam, Tanzania. Reg Environ Change 12(1):81–94. https://doi.org/10.1007/s10113-011-0239-4

Koehler J, Kuenzer C (2020) Forecasting spatio-temporal dynamics on the land surface using earth observation data—a review. Remote Sensing 12(21):3513. https://doi.org/10.3390/rs12213513

Kriegler E, Bauer N, Popp A, Humpenöder F, Leimbach M, Strefler J, Baumstark L, Bodirsky BL, Hilaire J, Klein D, Mouratiadou I, Weindl I, Bertram C, Dietrich J-P, Luderer G, Pehl M, Pietzcker R, Piontek F, Lotze-Campen H, Biewald A, Bonsch M, Giannousakis A, Kreidenweis U, Müller C, Rolinski S, Schultes A, Schwanitz J, Stevanovic M, Calvin K, Emmerling J, Fujimori S, Edenhofer O (2017) Fossil-fueled development (SSP5): an energy and resource intensive scenario for the 21st century. Glob Environ Change 42:297–315. https://doi.org/10.1016/j.gloenvcha.2016.05.015

Kumar V, Agrawal S (2022) Urban modelling and forecasting of landuse using SLEUTH model. Int J Environ Sci Technol (Tehran):1–20. https://doi.org/10.1007/s13762-022-04331-4

Kumar V, Sharma K, Caloiero T, Mehta D, Singh K (2023). Comprehensive overview of flood modeling approaches: a review of recent advances. Hydrology, 10(7). https://doi.org/10.3390/hydrology10070141

Kuo HF, Tsou KW (2017) Modeling and simulation of the future impacts of urban land use change on the natural environment by sleuth and cluster analysis. Sustainability 10(2). https://doi.org/10.3390/su10010072

Lee DR, Sallee GT (1970) A method of measuring shape. Geogr Rev 60(4):555–563. https://doi.org/10.2307/213774

Leimbach M, Kriegler E, Roming N, Schwanitz J (2017) Future growth patterns of world regions – a GDP scenario approach. Glob Environ Change 42:215–225. https://doi.org/10.1016/j.gloenvcha.2015.02.005

Li X, Gong P (2016) Urban growth models: progress and perspective. Sci Bull 61(21):1637–1650. https://doi.org/10.1007/s11434-016-1111-1

Liu X, Liang X, Li X, Xu X, Ou J, Chen Y, Li S, Wang S, Pei F (2017) A future land use simulation model (FLUS) for simulating multiple land use scenarios by coupling human and natural effects. Landsc Urban Plann 168:94–116. https://doi.org/10.1016/j.landurbplan.2017.09.019

Liu X, Wei M, Li Z, Zeng J (2022) Multi-scenario simulation of urban growth boundaries with an ESP-FLUS model: a case study of the min delta region, China. Ecological Indicators. 135. https://doi.org/10.1016/j.ecolind.2022.108538

Mahtta R, Fragkias M, Güneralp B, Mahendra A, Reba M, Wentz EA, Seto KC (2022) Urban land expansion: the role of population and economic growth for 300+ cities. npj Urban Sustainability 2(1). https://doi.org/10.1038/s42949-022-00048-y

Marconcini M, Metz-Marconcini A, Üreyen S, Palacios-Lopez D, Hanke W, Bachofer F, Zeidler J, Esch T, Gorelick N, Kakarla A, Strano E (2019) Outlining where humans live -- The World Settlement Footprint. arXiv e-prints 1910.12707.

Marconcini M, Metz-Marconcini A, Ureyen S, Palacios-Lopez D, Hanke W, Bachofer F, Zeidler J, Esch T, Gorelick N, Kakarla A, Paganini M, Strano E (2020) Outlining where humans live, the World Settlement Footprint 2015. Sci Data 7(1):242. https://doi.org/10.1038/s41597-020-00580-5

Marconcini M, Metz- Marconcini A, Esch T, Gorelick N (2021) Understanding current trends in global urbanisation - the World Settlement Footprint suite. Gi_forum 1:33–38. https://doi.org/10.1553/giscience2021_01_s33

Mård J, Di Baldassarre G, Mazzoleni M (2018) Nighttime light data reveal how flood protection shapes human proximity to rivers. Sci Adv 4(8):eaar5779. https://doi.org/10.1126/sciadv.aar5779

Merkens J-L, Reimann L, Hinkel J, Vafeidis AT (2016) Gridded population projections for the coastal zone under the shared socioeconomic pathways. Glob Planet Change 145:57–66. https://doi.org/10.1016/j.gloplacha.2016.08.009

Milanes CB, Martínez-González MB, Moreno-Gómez J, Saltarín J A, Suarez A, Padilla-Llano SE, Vasquez A, Lavell A, Zielinski S (2021) Multiple Hazards and Governance Model in the Barranquilla Metropolitan Area, Colombia. Sustainability 13(5). https://doi.org/10.3390/su13052669

Musa SI, Hashim M, Reba MNM (2016) A review of geospatial-based urban growth models and modelling initiatives. Geocarto Int 32(8):813–833. https://doi.org/10.1080/10106049.2016.1213891

Nardi F, Annis A, Di Baldassarre G, Vivoni ER, Grimaldi S (2019) Gfplain250m, a global high-resolution dataset of Earth's floodplains. Sci Data 6:180309. https://doi.org/10.1038/sdata.2018.309

Neal J, Hawker L, Savage J, Durand M, Bates P, Sampson C (2021) Estimating river channel bathymetry in large scale flood inundation models. Water Resour Res. 57(5). https://doi.org/10.1029/2020wr028301

Nicholls RJ, Cazenave A (2010) Sea-level rise and its impact on coastal zones. Science 328(5985):1517–1520. https://doi.org/10.1126/science.1185782

Nicholls RJ, Lincke D, Hinkel J, Brown S, Vafeidis AT, Meyssignac B, Hanson SE, Merkens J-L, Fang J (2021) A global analysis of subsidence, relative sea-level change and coastal flood exposure. Nat Clim Chang 11(4):338–342. https://doi.org/10.1038/s41558-021-00993-z

Nicholls RJ, Hanson S, Herweijer C, Patmore N, Hallegatte S, Corfee-Morlot J, Château J, Muir-Wood R (2008) Ranking Port Cities with High Exposure and Vulnerability to Climate Extremes: Exposure Estimates. Report No.: 19970900.

Nkwunonwo UC, Whitworth M, Baily B (2016) Review article: a review and critical analysis of the efforts towards urban flood risk management in the Lagos region of Nigeria. Nat Hazards Earth Syst Sci 16(2):349–369. https://doi.org/10.5194/nhess-16-349-2016

O'Neill BC, Tebaldi C, van Vuuren DP, Eyring V, Friedlingstein P, Hurtt G, Knutti R, Kriegler E, Lamarque J-F, Lowe J, Meehl GA, Moss R, Riahi K, Sanderson BM (2016) The scenario model intercomparison project (ScenarioMIP) for CMIP6. Geosci Model Dev 9(9):3461–3482. https://doi.org/10.5194/gmd-9-3461-2016

Onilude OO, Vaz E (2021) Urban sprawl and growth prediction for Lagos using GlobeLand30 data and cellular automata model. Sci 3(2):23. https://doi.org/10.3390/sci3020023

Park SH, Goo JM, Jo C-H (2004) Receiver operating characteristic (ROC) curve: practical review for radiologists. Korean J Radiol 5(1):11–18

Pelckmans I, Belliard J-P, Dominguez-Granda LE, Slobbe C, Temmerman S, Gourgue O (2023) Mangrove ecosystem properties regulate high water levels in a river delta. Nat Hazards Earth Syst Sci 23(9):3169–3183. https://doi.org/10.5194/nhess-23-3169-2023

Pirani A, Fuglestvedt JS, Byers E, O'Neill B, Riahi K, Lee J-., Marotzke J, Rose SK, Schaeffer R, Tebaldi C (2024) Scenarios in IPCC assessments: lessons from AR6 and opportunities for AR7. *npj Climate Action*, *3*(1). https://doi.org/10.1038/s44168-023-00082-1

Pontius RG, Schneider LC (2001) Land-cover change model validation by an ROC method for the Ipswich watershed, Massachusetts, USA. Agric Ecosyst Environ 85(1):239–248. https://doi.org/10.1016/S0167-8809(01)00187-6

Rafiee R, Mahiny AS, Khorasani N, Darvishsefat AA, Danekar A (2009) Simulating urban growth in Mashad City, Iran through the SLEUTH model (UGM). Cities 26(1):19–26. https://doi.org/10.1016/j.cities.2008.11.005

Randolph GF, Storper M (2022) Is urbanisation in the Global South fundamentally different? Comparative global urban analysis for the 21st century. Urban Stud 60(1):3–25. https://doi.org/10.1177/00420980211067926

Reguero BG, Losada IJ, Diaz-Simal P, Mendez FJ, Beck MW (2015) Effects of climate change on exposure to coastal flooding in Latin America and the Caribbean. PLoS ONE 10(7):e0133409. https://doi.org/10.1371/journal.pone.0133409

Reimuth A, Hagenlocher M, Yang LE, Katzschner A, Harb M, Garschagen M (2023) Urban growth modeling for the assessment of future climate and disaster risks: approaches, gaps and needs. Environ Res Lett. 19(1). https://doi.org/10.1088/1748-9326/ad1082

Riahi K, van Vuuren DP, Kriegler E, Edmonds J, O'Neill BC, Fujimori S, Bauer N, Calvin K, Dellink R, Fricko O, Lutz W, Popp A, Cuaresma JC, Kc S, Leimbach M, Jiang L, Kram T, Rao S, Emmerling J, Ebi K, Hasegawa T, Havlik P, Humpenöder F, Da Silva LA, Smith S, Stehfest E, Bosetti V, Eom J, Gernaat D, Masui T, Rogelj J, Strefler J, Drouet L, Krey V, Luderer G, Harmsen M, Takahashi K, Baumstark L, Doelman JC, Kainuma M, Klimont Z, Marangoni G, Lotze-Campen H, Obersteiner M, Tabeau A, Tavoni M (2017) The shared socioeconomic pathways and their energy, land use, and greenhouse gas emissions implications: an overview. Glob Environ Change 42:153–168. https://doi.org/10.1016/j.gloenvcha.2016.05.009

Rosenzweig C, Solecki W, Romero-Lankao P, Mehrotra S, Dhakal S, Bowman T, Ibrahim SA (2018).Climate Change and Cities: Second Assessment Report of the Urban Climate Change Research Network: Summary for City Leaders. In: Rosenzweig C, Romero-Lankao P, Mehrotra S, Dhakal S, Ali Ibrahim S, Solecki WD, editors. Climate Change and Cities: Second Assessment Report of the Urban Climate Change Research Network. Cambridge: Cambridge University Press; p. xvii-xlii

Saxena A, Jat MK (2020) Land suitability and urban growth modeling: Development of SLEUTH-Suitability. Comput Environ Urban Syst. 81. https://doi.org/10.1016/j.compenvurbsys.2020.101475

Schumann, G., Bates, P.D., Apel, H. and Aronica, G.T. (2018). Global Flood Hazard Mapping, Modeling, and Forecasting. In Global Flood Hazard (eds G.J.-P. Schumann, P.D. Bates, H. Apel and G.T. Aronica). https://doi.org/10.1002/9781119217886.ch14

Sett D, Trinh T, Wasim T, Ortiz-Vargas A, Nguyen DGC, Büche K, Assmann A, Nguyen HKL, Walz Y, Souvignet M, Bachofer F, Vu TB, Garschagen M, Hagenlocher M (2024) Advancing understanding of the complex nature of flood risks to inform comprehensive risk management: Findings from an urban region in Central Vietnam. Int J Disaster Risk Reduct 110:104652. https://doi.org/10.1016/j.ijdrr.2024.104652

Silverman BW (1986). Density estimation for statistics and data analysis. 1. publ. ed. London [u.a.]: Chapman and Hall

Srichaichana J, Trisurat Y, Ongsomwang S (2019) Land use and land cover scenarios for optimum water yield and sediment retention ecosystem services in Klong U-tapao watershed, Songkhla, Thailand. Sustainability 11(10):2895

Strauss BH, Kulp SA, Rasmussen DJ, Levermann A (2021) Unprecedented threats to cities from multi-century sea level rise. Environ Res Lett. 16(11). https://doi.org/10.1088/1748-9326/ac2e6b

Sun Q, Fang J, Dang X, Xu K, Fang Y, Li X, Liu M (2022) Multi-scenario urban flood risk assessment by integrating future land use change models and hydrodynamic models. Nat Hazards Earth Syst Sci 22(11):3815–3829. https://doi.org/10.5194/nhess-22-3815-2022

Susetyo C, Yusuf L, Setiawan RP (2022) Spatial planning concept for flood prevention in the Kedurus River watershed. Open Geosci 14(1):1238–1249. https://doi.org/10.1515/geo-2022-0421

Tate E, Rahman MA, Emrich CT, Sampson CC (2021) Flood exposure and social vulnerability in the United States. Nat Hazards 106(1):435–457. https://doi.org/10.1007/s11069-020-04470-2

Taylor KE, Stouffer RJ, Meehl GA (2012) An overview of CMIP5 and the experiment design. Bull Am Meteorol Soc 93(4):485–498. https://doi.org/10.1175/bams-d-11-00094.1

Tellman B, Sullivan JA, Kuhn C, Kettner AJ, Doyle CS, Brakenridge GR, Erickson TA, Slayback DA (2021) Satellite imaging reveals increased proportion of population exposed to floods. Nature 596(7870):80–86. https://doi.org/10.1038/s41586-021-03695-w

Terama E, Clarke E, Rounsevell MDA, Fronzek S, Carter TR (2017) Modelling population structure in the context of urban land use change in Europe. Reg Environ Change 19(3):667–677. https://doi.org/10.1007/s10113-017-1194-5

UNEP-WCMC, IUCN (2023) Protected Planet: The World Database on Protected Areas (WDPA). In: UNEP-WCMC and IUCN, editor. Cambridge, UK

UNFCCC (2015) Adoption of the Paris Agreement. Report No. FCCC/CP/2015/L.9/Rev.1. http://unfccc.int/resource/docs/2015/cop21/eng/l09r01.pdf. Accessed 19.03.2025.

van Vuuren DP, Edmonds J, Kainuma M, Riahi K, Thomson A, Hibbard K, Hurtt GC, Kram T, Krey V, Lamarque J-F, Masui T, Meinshausen M, Nakicenovic N, Smith SJ, Rose SK (2011) The representative concentration pathways: an overview. Clim Change 109(1–2):5–31. https://doi.org/10.1007/s10584-011-0148-z

van Vuuren DP, Kriegler E, O'Neill BC, Ebi KL, Riahi K, Carter TR, Edmonds J, Hallegatte S, Kram T, Mathur R, Winkler H (2013) A new scenario framework for climate change research: scenario matrix architecture. Clim Chang 122(3):373–386. https://doi.org/10.1007/s10584-013-0906-1

van Vuuren DP, Stehfest E, Gernaat DEHJ, Doelman JC, van den Berg M, Harmsen M, de Boer HS, Bouwman LF, Daioglou V, Edelenbosch OY, Girod B, Kram T, Lassaletta L, Lucas PL, van Meijl H, Müller C, van Ruijven BJ, van der Sluis S, Tabeau A (2017) Energy, land-use and greenhouse gas emissions trajectories under a green growth paradigm. Glob Environ Chang 42:237–250. https://doi.org/10.1016/j.gloenvcha.2016.05.008

Varquez ACG, Darmanto N, Kawano N, Takakuwa S, Kanda M, Xin Z (2017) Representative urban growing scenarios for future climate models. J Japan Society Civil Eng Ser B1 (Hydraulic Engineering) 73(4):I_103-I_108. https://doi.org/10.2208/jscejhe.73.I_103

Verburg PH, Overmars KP (2009) Combining top-down and bottom-up dynamics in land use modeling: exploring the future of abandoned farmlands in Europe with the Dyna-CLUE model. Landsc Ecol 24(9):1167–1181. https://doi.org/10.1007/s10980-009-9355-7

Verburg PH, Soepboer W, Veldkamp A, Limpiada R, Espaldon V, Mastura SSA (2002) Modeling the spatial dynamics of regional land use: the CLUE-S model. Environ Manage 30(3):391–405. https://doi.org/10.1007/s00267-002-2630-x

Verburg PH, de Nijs TCM, Ritsema van Eck J, Visser H, de Jong K (2004) A method to analyse neighbourhood characteristics of land use patterns. Comput Environ Urban Syst 28(6):667–690. https://doi.org/10.1016/j.compenvurbsys.2003.07.001

Wang Z, Bachofer F, Koehler J, Huth J, Hoeser T, Marconcini M, Esch T, Kuenzer C (2022) Spatial modelling and prediction with the spatio-temporal matrix: a study on predicting future settlement growth. Land 11(8):1174. https://doi.org/10.3390/land11081174

Wang S, Zhang HJ, Wang TT, Hossain S (2024) Simulating runoff changes and evaluating under climate change using CMIP6 data and the optimal SWAT model: a case study. Sci Rep 14(1):23228. https://doi.org/10.1038/s41598-024-74269-9

Wing OEJ, Bates PD, Sampson CC, Smith AM, Johnson KA, Erickson TA (2017) Validation of a 30 m resolution flood hazard model of the conterminous United States. Water Resour Res 53(9):7968–7986. https://doi.org/10.1002/2017wr020917

Winsemius H, Ward P, Luo T (2015) Aqueduct Global Flood Risk Maps Washington, DC, USA: World Resources Institute. Available from: https://www.wri.org/data/aqueduct-global-flood-analyzer. Accessed 28.08.2023
Wolff C, Nikoletopoulos T, Hinkel J, Vafeidis AT (2020) Future urban development exacerbates coastal exposure in the Mediterranean. Sci Rep 10(1):14420. https://doi.org/10.1038/s41598-020-70928-9
Wolff C, Bonatz H, Vafeidis AT (2023) Setback zones can effectively reduce exposure to sea-level rise in Europe. Sci Rep 13(1):5515. https://doi.org/10.1038/s41598-023-32059-9
World Bank (2014) Turn Down the Heat: Confronting the New Climate Normal. Washington, DC: World Bank. Contract No.: 92704 v3.
WRI Aqueduct (2023) Aqueduct Global Flood Analyzer: World Resources Institute (WRI). Available from: https://www.wri.org/applications/aqueduct/floods/. Accessed 28.12.2023
Wu X, Hu Y, He HS, Bu R, Onsted J, Xi F (2008) Performance evaluation of the SLEUTH model in the Shenyang Metropolitan Area of Northeastern China. Environ Model Assess 14(2):221–230. https://doi.org/10.1007/s10666-008-9154-6
Yeh AGO, Li X, Xia C (2021).Cellular Automata Modeling for Urban and Regional Planning. In: Shi W, Goodchild MF, Batty M, Kwan M-P, Zhang A, editors. Urban Informatics. Singapore: Springer Singapore; p. 865–883
Zhou Y, Varquez ACG, Kanda M (2019) High-resolution global urban growth projection based on multiple applications of the SLEUTH urban growth model. Sci Data 6(1):34. https://doi.org/10.1038/s41597-019-0048-z